A METHOD OF ENRICHMENT OF THE ENDOPLASMIC RETICULUM AND GOLGI COMPLEX PROTEINS FROM WHEAT SEEDS (*TRITICUM AESTIVUM*) AT DIFFERENT STAGES OF GROWTH

By

MOHAMAD AREF EL-OSTA

Bachelor of Science
American University of Beirut
Beirut, Lebanon
1991

Master of Science
Oklahoma State University
Stillwater, Oklahoma
1999

Submitted to the Faculty of the
Graduate College of the
Oklahoma State University
in partial fulfillment of
the requirement for
the Degree of
DOCTOR OF PHILOSOPHY
May 2005

A METHOD OF ENRICHMENT OF THE ENDOPLASMIC RETICULUM AND GOLGI COMPLEX PROTEINS FROM WHEAT SEEDS (*TRITICUM AESTIVUM*) AT DIFFERENT STAGES OF GROWTH

Thesis Approved:

Dr. Patricia Rayas-Duarte

Thesis Advisor

Dr. Andrew Mort

Dr. Jose Soulages

Dr. Mikael Anderson

A. Gordon Emslie

Dean of the Graduate College

ACKNOWLEDGMENTS

I would like to express my sincere appreciation to my supervisor, Dr. Patricia Rayas-Duarte for granting me the opportunity to improve my carrier skills in the current project. My experience with her as a supervisor shall always remain a landmark in my life. Apart from her thorough scientific surveillance, I would like to highlight her encouragement, inspiration and personal friendship with my family during the years I worked with her.

I would like also to show my thanks and appreciations to my Doctoral committee members, Dr. Jose Soulages, Dr. Andrew Mort and Dr. Michael Anderson for their professional guidance and help.

A special appreciation is also expressed to Dr. Steve Hartson and the team of the Recombinant DNA/Protein Resource Facility at Oklahoma State University, Department of Biochemistry and Molecular Biology. Without Dr. Hartson's guidance, assistance and innovations, this project certainly could not meet the expectations. I would like also to show my deepest gratitude to the Department of Biochemistry and Molecular Biology, the Food and Agriculture Product Research Center, and the Howard Huges Medical Institute, for the generous financial assistance and academics I received during my work.

Last, in this moment, I would like to remember the people who supported me during the moments I truly needed support, namely my wife Suzane to whom I express my deepest love and cherish, my father Dr. Aref who was always my inspirer for a higher

academic achievement and also my mother Huda for her prayers and encouragement. I want also to thank them for being non-hesitating helpers during the time of financial hardship.

TABLE OF CONTENTS

Chapter Page

I LITERATURE REVIEW……...…… 1

INTRODUCTION…… 2

RATIONAL FOR SELECTING ORGANELLES PROTEOMIC AS A MARKER FOR STORAGE PROTEIN QUALITY…….……3

ENDOSPERM ANATOMY AND STAGES OF DEVELOPMENT…….. 3

STORAGE PROTEIN BIOSYNTHESIS WITHIN THE SECRETORY PATHWAY…….. 5

a. Description of Storage Proteins……..…… 5

b. Structure of Constitutive proteins in the Secretory Pathway……. 6

c. ER Structure and Organization……...… 8

d. Lumenal Continuity of the ER……9

e. Post-translational Modification and Retention of Storage Protein in the ER……...……... 9

f. ER-Golgi Transport of Storage Protein……...14

g. Transient Status of the Pre-Golgi Intermediates……..……15

h. Golgi Complex Structure……16

i. ER-Golgi Protein Cycling……...…… 18

MORPHOLOGICAL CHANGES IN THE MEMBRANE SYSTEM DURING DIFFERENT STAGES OF GRAIN DEVELOPMENT…….…. 19

EVIDENCE OF TEMPORAL EXPRESSION OF CONSTITUTIVE PROTEINS AT DIFFERENT STAGES OF GRAIN DEVELOPMENT… 20

STORAGE PROTEIN FINAL DISTRIBUTION AND CHARACTERISTICS…….. 22

LITTERATURE CITED…….……..23

Chapter Page

II A METHOD OF ENRICHMENT OF THE ENDOPLASMIC RETICULUM AND GOLGI COMPLEX PROTEINS FROM WHEAT SEEDS (*TRITICUM AESTIVUM*) AT DIFFERENT STAGES OF GROWTH……. 28

INTRODUCTION……..……..……29

MATERIALS AND METHODS……..……..……...…33
Procedures for Wheat Seeds Growth……..… 33
Growth Curve: Weight of Seeds Vs Time……..…….33
Fractionation of the ER and GC…….……33
Two Phase Partitioning…….……36
Separation of Smooth and Rough ER……..…….....….37
Ribosome Stripping from rough ER……..…….....37
Quantitative Protein Determination by BCA……38
SDS-PAGE……..……..…...38
Immunodetection of the ER and GC Enzyme Markers ……..……39
2-D Electrophoresis……..……40
Peptide Mass Fingerprinting Using MALDI-TOF ……41

RESULTS…….……43
Weight Change of Wheat Seeds versus Time.……..…….....43
Protein Recovery ……..…….....43
Protein Patterns from the Enrichment Steps…….……..45
Western Blot for Enzyme markers of Organelles…….. 50
Descriptive Analysis of Enriched Organelles Proteins Visualized by the 2-D Elecrophoresis and MALDI-TOF …… 50

DISCUSSION……..……..... 56
Evaluation of the Weight Change Curve of Wheat Seeds during the Four Stages of Growth……...…… 57
Evaluation of Protein Recovery Rates during Fractionation…… 57
Optimization of the Two Phase Partitioning ……..... 62
Evaluation of the Sucrose Fractionation Method……...64
Results of Proteins Resolving by 2-D Electrophoresis and MALDI-TOF……..……...……... 72
CONCLUSION …….……..……..…….…….. 81

FUTURE RECOMMENDATION……. 84
ACKNOWLEDGMENTS……..……..……86

LITTERATURE CITED…….…...……..87

III APPENDICES…….....…….....103
VITA
ABSTRACT

APPENDICE A

LIST OF TABLES

Table Page

1 Protein recovery of endoplasmic reticulum (ER) and Golgi complex (GC) enrichment from developing wheat endosperm……..……...106
2 Results of database search of protein spots identified by MALDI-TOF from whea endosperm organelles during development…….....107

APPENDICE B

LIST OF FIGURES

Figure		Page
1	Pattern of weight change of wheat endosperm during development analyzed at 4 stages of growth ……..…….….....	113
2	SDS-PAGE showing the pattern of organelles enrichment at the 4 stages of wheat development…….....	114
3	Western blot analysis of endoplasmic reticulum (ER) and the Golgi complex (GC) enrichment extract from developing wheat endosperm..	115
4	2-D separation of enriched organelles fraction at different stages of growth……....	116
5	5 Chart illustrating different steps of the fractionation and enrichment stages of ER and GC from wheat endosperm…….	124

ABBREVIATIONS

ACN	Acetonitrile
BCA	Bicinchoninic Acid
BCIP/NBT	Bromochloroindolyl Phosphate/Nitro Blue Tetrazolium
BSA	Bovine Serum Albumin
CCV	Clathrin Coated Vesicles
CHAPS	[(3-Cholamidopropyl) Dimethylammonio]-1-Propane Sulphonate
CRT	Calreticulin
DAA	Days After Anthesis
DEX	Dextran
DTT	Dithiothreitol
EDTA	Ethylenediaminetetraacetic Acid
En	Enriched
ER	Endoplasmic Reticulum
FTCD	Formiminotransferase Cyclodeaminase
HEPES	N-(2-Hydroxyethyl) Piperazine-N'-(2-Ethanesulfonic Acid)

HMW	High Molecular Weight
HPLC	High Performance Liquid Chromatography
IEF	Isoelectric-Focusing
IPG	Immobilised pH Gradient Strips
KCl	Potassium Chloride
LMW	Low Molecular Weight
MALDI-TOF	Matrix Assisted Laser Desorption Ionization-Time of Flight
PB	Protein Bodies
PEG	Polyethylene Glycol
PGCs	Post-Golgi Carriers
PDI	Protein Disulfide Isomerase
PPI	Peptidyl-Prolyl *cis-trans* Isomerases
RT	Room Temperature
SDS-PAGE	Sodium Dodecyl Sulfate-Polyacrylamide Gel Electrophoresis
TFA	Trifluoroacetate
TGN	*Trans* Golgi Network
TMD	Transmembrane Domain

CHAPTER I

LITERATURE REVIEW

INTRODUCTION

The bread-making quality of wheat has been largely attributed to storage proteins. Storage proteins are known to be processed in secretory membranes connected to storage vacuoles. Storage proteins are usually vacuolar; but several cereals, including wheat, utilize the endoplasmic reticulum (ER) to accumulate their storage protein into large aggregates termed protein bodies (PB). Numerous previous studies speculated that changes in the secretory membrane protein profiles are related to changes in the quality of the storage protein processed inside. The secretory membrane system allows cells to regulate delivery of newly synthesized proteins, carbohydrates, and lipids to the vacuolar storage system or to the cell surface, which is necessary for growth and homeostasis. The secretory pathway is made up of distinct organelles including the ER, Golgi complex, plasma membrane, and tubulovesicular transport intermediates that mediate intracellular membrane transport among them (1).

All seed-storage proteins are secreted into the ER, where the transit peptide is removed and other posttranslational processing, such as chaperone-assisted folding, may take place. Some wheat-storage proteins then appear to follow the secretory pathway from ER to Golgi and then to storage vacuoles. However, other proteins accumulate in the ER and then are incorporated into vacuole-like compartments that transform into PB. There are no recognizable PB in the endosperm of the mature wheat grain, and this feature seems exclusive to wheat during the growth stages. Instead, during the mature stage, protein in the vacuole-like compartments is compressed between the starch granules (1).

RATIONAL FOR SELECTING ORGANELLE PROTEOMICS AS MARKERS FOR STORAGE PROTEIN QUALITY

In the past years, the breeding efforts for improving wheat quality were concentrated mainly at the gene level. However, information from the research at the gene level does not necessarily match that at the protein level, quantitatively or qualitatively. Biological and biochemical phenomena, including protein structural stability and half-life; modifications of proteins at the post-transcriptional, co-translational and degradative levels; and the involvement of environmental factors, affect the gene products. This has led to a conclusion that there is no strict linear relationship between genes and the protein complements of a cell. Consequently, knowledge of genotype alone does not illustrate the changes in grain quality due to numerous complex-factor fluctuations. This information can be provided at the biochemical level by detailed analysis of protein composition, since this particular protein composition is the result of gene expression under specific conditions (2).

ENDOSPERM ANATOMY AND STAGES OF DEVELOPMENT

The wheat grain is composed of different tissues. Briefly, the mature grain is made of a caryopsis, with an outer testa closely appended to the seed. The seed includes the outer maternal pericarp layer, the embryo, and the endosperm. The endosperm is made of two main parts: an outer aleurone layer and inner endosperm cells in the form of columns of starch. Milling removes the embryo, aleurone, and pericarp plus testa, leaving the starchy endosperm as the principal contributor to white flour (3).

Stages of endosperm development begin with the fertilization of a diploid cell followed by repeated division of the triploid nuclei, and finally a gradual formation of cell walls. This is the stage of cellular division (4).

The next stage is a period of cellular expansion during which water content increases and starch and protein reserves accumulate. The maximum amounts of starch and protein that accumulate in each grain depend on the number of endosperm cells, determined early in grain fill; and on the final size of the cells, which is influenced by water uptake, cell-wall extensibility, and the rate and duration of grain fill, all of which are affected by growth conditions. Cellular expansion and water accumulation stop at early mature stages. However, dry-matter accumulation continues where starch and protein replace cell water, and the kernel begins to desiccate until late-mature stages (3).

In the latest stages of development, the formation of a waxy layer at the chalaza (zone of entry into the grain) interferes with the input of sugars and amino acids into the grain (5). This is the stage where the seeds reach physiological maturity in which the protein and starch deposits cease, and the grain reaches maximum dry weight. At approximately this time the endosperm tissue undergoes a form of apoptosis, or programmed cell death (6). Aleurone is the only cell part that remains viable, whereas the kernels desiccate rapidly, keeping only 10–15% of their water content, at which time they are ready for harvest (7).

STORAGE PROTEIN BIOSYNTHESIS WITHIN THE SECRETORY PATHWAY

a. Description of Storage Proteins

The protein gluten constitutes a class of interrelated storage proteins called the prolamins. Their structure allows for tight packing and high stability. Prolamins are present only in cereal seeds and are characterized by their solubility in alcohol and their insolubility in water. The only function of the prolamins in plants is to store nitrogen, carbon and sulfur for mobilization during germination. However, in wheat dough the prolamins form a three-dimensional network, called gluten, responsible for the visco-elastic properties that allow wheat flour to be processed into yeasted bread and a range of other by-products. Wheat gluten comprises over 50 individual proteins, all of which contain domains based on repeated sequences. However, one group, called the high molecular weight (HMW) glutenin subunits, appears to be the main determinant of gluten elasticity (8).

The prolamins are highly polymorphic mixtures of components with molecular weight values of 30 to 90 kDa. These prolamins are classified based on their amino acid sequences into three groups: the S-rich, S-poor, and the most interesting, HMW glutenin subunits. The S-rich prolamins are the major prolamins group, accounting for 80 to 90% of the total prolamins fractions. They include polymeric units containing interchain disulfide bonds and monomeric units containing intrachain disulfide bond components, all consisting of the α-gliadins, γ-gliadins, and low-molecular-weight (LMW) glutenin subunits. Their amino acid sequences consist of two separate domains: an N-terminal domain composed of repeated sequences, and a nonrepetitive C-terminal domain. The S-

poor prolamins include the ώ-gliadins. They cannot form oligomers or polymers because they generally lack cysteine residues (9).

The HMW glutenin determines the elasticity of wheat dough, which in turn determines the bread-making quality. HMW prolamins have extensively repeated sequences flanked by nonrepetitive N- and C-terminal domains. In many units the repeated sequences are based on the motifs Gly-Tyr-Tyr-Pro-Thr-Ser-Pro or Leu-Gln-Gln, Pro-Gly-Gln-Gly-Gln-Gln, and in some subunits only, Gly-Gln-Gln (9).

Globulins constitute only a fractional amount of the storage proteins in wheat. Based on their sedimentation coefficients, they can be divided into two groups: the 7S globulins and the 11S globulins. The 7S globulins are trimeric proteins with a molecular weight of 150 to 190 kDa, lacking the cysteine residues necessary to form disulfide bonds. The 11S proteins consist of six subunit pairs that interact noncovalently. Each of these subunit pairs consists in turn of an acidic subunit of 40 kDa and a basic subunit of 20 kDa linked by a single disulfide bond. Each subunit pair is synthesized as a precursor protein that is proteolytically cleaved after disulfide-bond formation (9).

b. Structure of Constitutive Proteins in the Secretory Pathway

The membrane system is a major part of the constitutive protein of the secretory pathway. The membrane system is composed of interfacial regions about 15 Å thick each and the hydrocarbon core, which has a thickness of about 30 Å. Various parts of the peripheral proteins interact with both of these regions. Only two structural motifs have been observed for membrane proteins: membrane-spanning α-helix bundles and β-

barrels, with the former being predominant. A frequently observed submotif is interfacial helices connected to adjacent transmembrane helices (10).

Generally, the interior amino acids are mostly nonpolar and packed as tightly as those of soluble proteins. Salt-bridges play an important key role in some transport proteins. The interiors of membrane proteins are comprised of internally H-bonded α-helices and β-sheets. Major portions of their masses are buried within the hydrocarbon core of the membrane and arranged so that their outer surfaces face these cores. Although the average hydrophobicity of the interiors of membrane proteins is the same as for soluble proteins, the amino acids of these outer surfaces are more hydrophobic (10).

i. Assembly of Constitutive Protein within the Membrane System

Constitutive membrane proteins are assembled via a complex translocation/insertion mechanism. In brief, the ribosome secretes nascent chains into membrane-resident translocons, where they are assembled and released into the membrane (10).

The structure of the ER translocon is reported to be a doughnut-like structure with a central pore spanning the entire ER membrane. During its active state the ER translocon is aligned with the large ribosomal subunit to facilitate the pathway of nascent polypeptide chains toward the site of ER translocation (11). After completion of the process, the ribosome-translocon complex dissociates, leaving the protein stably folded in the membrane (10).

Nonconstitutive membrane proteins bypass this elaborate machinery by spontaneously entering the membrane from the aqueous phase. They do this by existing as soluble forms in the aqueous phase and then binding to membranes (11).

ii. Role of Fluid Lipid Bilayers in the Structural Protein Assembly

The major role of the hydrophobicity in membrane protein is to favor the establishment of secondary structural elements across the lipid bilayer. The structure of the fluid bilayer consists of spatial distributions of the structural groups of lipids (carbonyls, phosphates, etc) and water, projected onto an axis normal to the bilayer plane. In addition, the interfaces are chemically heterogeneous, in such a way that they are rich in noncovalent interactions with peptides. Because the interfaces are the sites of first contact, they are especially important in the folding and insertion of membrane proteins (11).

c. ER Structure and Organization

The ER is the starting point of the outbranched secretory pathway. It is the largest intracellular compartment, associated with an extensive network of interconnecting membrane tubules extending through the cell. The ER consists of a network of continuous tubules and flattened sacs extended in the cytoplasm and connected to the nuclear envelope, but remain distant from the plasma membranes. The ER membranes are physiologically active and contain differentiated domains specialized for distinct functions. These functions include protein folding, assembly and degradation, lipid metabolism, and membrane transport (12).

Secretory cargo is synthesized and assembled in the ER and then, depending on the growth stage, may either reside locally or, alternatively, may leave the ER via distinct exit sites that bud and translocate as tubulovesicular structures (pre-Golgi) toward the microtubules. At this point, the destination is to merge with Golgi membranes for further processing and maturation. Upon arrival at the *trans*-Golgi network (TGN), which is the distal Golgi part, proteins are sorted and packaged into post-Golgi carriers that move through the cytoplasm in microtubules to reside in storage vacuoles or to fuse with the cell surface. This unidirectional membrane flow is balanced by retrieval pathways that recycle membranes and selected proteins back to their original compartments (12).

d. Lumenal Continuity of the ER

ER membranes are reported as being differentiated into rough and smooth regions, depending on whether ribosomes are associated with their cytoplasmic surfaces. Whereas the rough ER is the site of cotranslational membrane insertion of proteins, the smooth ER is thought to be the site of lipid biosynthesis, detoxification, and calcium regulation. However, fluorescence-tagging techniques have revealed that the membranes and lumenal spaces of the ER are continuous throughout the cell and that both ER membranes form an interconnected system (13, 14).

e. Post-translational Modification and Retention of Storage Protein in the ER

***i.* Post Translational Assembly**

After their secretion, proteins assume their folded conformations within the ER lumen. More than one type of ER lumenal protein may assist in these processes, which are necessary for protein maturation and oligomerization. Molecular chaperones of the

HSP70/BiP family are reported to have a dual role in the ER lumen. They may facilitate folding by binding transiently to the nascent polypeptides, preventing early inappropriate folding. They may also prevent the formation of incorrect inter- or intramolecular interactions. A second group of proteins, the peptidyl-prolyl *cis-trans* isomerases (PPI) or cyclophilins, of which one subclass (the S-cyclophilins) is resident in the ER lumen, may also assist in the folding (9).

The 7S and 11S globulin subunits are assembled and folded in the ER. The assembly of the 11S globulins is a highly regulated event. The monomeric proteins are initially assembled in the ER lumen into trimers, but are then transported from the ER to the storage vacuoles, where they are assembled into their final hexameric form. This assembly process requires specific proteolytic cleavage of the subunits present in the trimers (8). Globulin (triticin) inclusions are present within a prolamin matrix in wheat. In contrast, different types of prolamins are spatially separated in the protein bodies of cereal endosperms (9).

ii. Disulfide Bond Formation during Folding in ER

The ER is the site of disulfide bond formation. The assembly of some prolamins into disulfide-stabilized polymers takes place in the ER (9). The levels of protein disulfide isomerase (PDI) transcripts increase earlier than those of gluten proteins (15).

PDI is associated with the ER in developing wheat endosperms (15). It is a multifunctional glycoprotein involved in the formation and isomerization of disulfide bonds in nascent secretory proteins. PDI also assists in a variety of protein-maturation processes within the ER. In addition to its primary role in disulfide bond formation, PDI

is also the P-subunit of prolyl-4-hydroxylase that adds hydroxyl groups to some secretory proteins. Plants contain a variety of vacuolar proteins containing disulfide bonds whose folding is assisted by PDI. These include storage proteins, hydrolases, proteases, and α-amylase inhibitors, as well as enzymes involved in plant defense. The S-rich gliadin contain six to eight Cys residues that are located in the C-terminal region and are linked by three to four intramolecular disulfide bonds assisted by PDI (16).

iii. Retention

Retention of Storage Protein

It was reported that, following entrance into the ER, storage proteins initiate a slow process of aggregation, and the aggregation state will dictate the pathway taken afterward. At earlier stages of grain-filling (14-20 DAA), more protein may escape aggregation within the ER, transport to the Golgi, sequester into PB, and later be transported to small or large vacuoles (17). However, during maturation of the endosperm cells, protein aggregation intensifies. This will eventually lead to the formation of aggregates in the form of small vacuoles within the ER lumen. These small vacuoles may further fuse to form, finally, a central vacuole in which the PB are sequestered. These PB apparently continue to enlarge by fusions with each other inside the vacuoles (18).

The continuous fusion leads to PB growing in size, mostly by continuous deposition of storage proteins, forming large PB surrounded by the ER. This process of PB fusion and enlargement causes rupture and discontinuity of the ER membrane around the PB. The mechanism by which the ER-surrounded PB in the cytoplasm enter distant storage vacuoles is not understood. PB are much larger than the Golgi complex,

consequently this organelle is less likely to be involved in their transport. In addition, it is not clear whether all of these PB subsequently enter vacuoles, as it is difficult to detect vacuoles at this stage (19).

One theory suggested that the prolamin-repetitive domains could be responsible for storage-protein retention within the ER by interacting with ER components, while another theory suggested that interactions between individual prolamin molecules result in the formation of insoluble aggregates that are retained within the ER lumen. The latter theory is supported by the observation that rice prolamin mRNAs are segregated to a distinct region of the rough ER, which allows aggregation of the prolamins to occur in localized parts of the ER, preventing widespread effects on ER integrity (9).

Retention of Membranes Proteins

Soluble Proteins

Soluble resident proteins in the ER are distinguished from cargo protein by a retention signal, which is a tetrapeptide containing H/KDEL at the C-terminal end. The resident proteins holding this tetrapeptide are collectively referred to as reticuloplasmin. In addition to its role as an ER retention signal, HDEL could be involved in targeting chaperone misfolded protein complexes that escape the ER towards the lytic vacuoles.

In yeast, two HDEL-specific receptors have been identified: ERD1 and ERD2. The latter is a 26 kDa protein responsible for the backward transport of escaping proteins from the early Golgi compartment to the ER. The recycling receptors are located in the post-ER compartment and throughout the Golgi. This escape is short-distanced in plants,

shown by a lack of Golgi-modified recycled proteins. Calreticulin is the best example of an ER-resident protein lacking the N-glycosylation type of Golgi modification (11).

Insoluble Proteins

Specific signals are necessary to retain resident integral membrane proteins within the ER or the Golgi membranes. A cytosolic di-lysin motif has been identified at the C-terminal end of many type-I integral membrane proteins that reside in the ER of yeast. This sequence is sufficient for integral membrane-protein retention in the ER. As for soluble ER protein containing H/KDEL, the C-terminal di-lysin motif mediates the recycling of type I membrane proteins from the Golgi back to the ER. For the type II membrane protein, a double arginine motif at the N-terminus is presumed to be a retrieval signal in the ER. Calnexin is an abundant membrane protein that works as a chaperone transiently binding to nascent glycoproteins. However, calnexin doesn't have a di-lysin motif in its C-terminal like regular type I membrane proteins; rather, it contains a di-argenine motif like the type II membranes (20).

The ER plays an important dual role in the transportation of a part of correctly folded proteins into the secretory pathway and in retention because incorrectly folded proteins and a part of assembled proteins are respectively degraded or retained in this compartment. It is most likely that stress resulting from heat or drought will affect the folding chaperone, which eventually results in loss of exported protein quality. When interactions between misfolded protein and chaperone become irreversible, the mobility of proteins in the ER becomes restricted, leading to proteins retention or degradation (21).

f. The ER-Golgi Transport of Storage Protein

There are two routes of PB formation operating in developing wheat endosperm. In one of them the PB form from vacuoles and in the other the PB form from the ER (1).

Regarding globulins, the 11S globulin is transported from the ER lumen via the Golgi apparatus to the vacuole. The fragmentation of the vacuoles then forms PB. The 7S albumins and the 11S globulins of legumes and other dicots are transported via the Golgi apparatus to the vacuole, which fragments to form PB (9).

In contrast, the prolamins appear to be mostly retained within the lumen of the ER, which form PB. Consequently, the endosperm cells contain two populations of PB, some of vacuolar origin and others of ER origin (9). Glutenins are retained in ER-derived PB, whereas gliadins are present in both types of PB.

Regarding the Golgi-mediated transport route, following proper folding and oligomer assembly, newly synthesized proteins destined for secretion are selectively separated from ER-resident proteins. This occurs at ER exit sites, which are entities scattered over the ER surface. These exits are highly organized membrane domains containing multiple budding vesicles that subsequently fuse to form pre-Golgi transport intermediates (19).

Exit-site domains have an increased level of organization of proteins and lipids compared with surrounding ER membranes. The export sites contain the coating-protein complex (COPII), which is specialized in export from ER toward Golgi. It is composed of an ER luminal protein Sar1 and two cytosolic heterodimer proteins, including the nucleotide exchange factor sec12. COPII assembly onto membranes at ER exit sites is initiated with Sec12-mediated nucleotide exchange of GTP (in place of GDP) onto Sar1,

with cargo molecule receptors triggering this exchange. Sec23/24 and Sec13/31 heterodimers are sequentially assembled onto the cytoplasmic side of the ER membrane to form a COPII-coated bud. This bud is generally thought to then transform into a vesicle (22).

ER exit sites are stable and dynamic structures that can rapidly reorganize in response to trafficking interference. However, ER exit sites are not consumed by the formation and translocation of pre-Golgi transport intermediates. Rather they are *de novo* synthesized in the ER due to reverse shipment toward the ER (23).

g. Transient Status of the Pre-Golgi Intermediates

When COPII-coated proteins are concentrated at ER exit sites, those sites are involved in one of two phenomena. They may first engage in repeated vesicle budding and delivery to pre-Golgi intermediates. Alternatively, they could directly transform into tubular membrane clusters. The observation that pre-Golgi structures move away from ER exit sites leads to the suggestion that these intermediates are constantly de-novo generated at these sites rather than existing there as stable intermediary compartments. Furthermore, Pre-Golgi structures seem to fuse with the Golgi complex following transport. All of those facts lead to the suggestion that pre-Golgi intermediates have only a transient existence initiated in ER exit sites, and that they may be involved in sorting and recycling selected components back to the ER (24).

COPI is a heptameric cytosolic protein complex that assembles onto Golgi membranes to form a coat that facilitates budding and fission of transport intermediates. A suggested role for COPI is as a mediator for the budding of retrograde vesicles, which would recycle proteins either backward to the ER or from late to early Golgi

compartments. In fact, it was reported that the ER-exit-site membrane becomes first differentiated by COPII, and then, by COPI association, coming from Golgi, which further helps maturation of COPII-derived ER exit sites (25). This was demonstrated by the fact that, in the absence of COPI activity, the action of Sar1/COPII is insufficient to sort protein into pre-Golgi intermediates**.** This would suggest that COPI binding is required for maintaining secretory molecules in pre-Golgi as well as in Golgi elements (26).

h. Golgi Complex Structure

The Golgi complex occupies a central position in the secretory pathway. The term Golgi complex refers to the apparatus comprising the Golgi stacks, the TGN and the Golgi matrix, all dispersed within the cytoplasm. Each stack consists of a set of five to eight flattened cisternae. The TGN shows a tubulovesicular structure and is always closely associated with the trans-side of the stack. The Golgi matrix is a fine-filamentous structure with a speculated role of protecting stacks from shearing and preventing the loss of transport vesicles from the stacks (27).

Within the cytoplasm, the Golgi is the site where proteins and lipids are modified and sorted. Furthermore, and the Golgi acts as a filter to segregate proteins and lipids to be retained in the ER/Golgi system from those to be delivered to the plasma membrane. It is also a factory for the production of complex carbohydrates (12).

Targeting and localizing of integral membrane proteins to the Golgi is due either to cytoplasmic tail-based targeting determinants and/or transmembrane domain (TMD). Furin, a residing membrane protein found in the TGN is targeted by a tyrosine-containing

sequence in its cytoplasmic tail. Its retention in the TGN involves two independent targeting signals. The first is an acidic peptide TMD for localization in the Golgi and the second is a tetrapeptide for the retrieval signal of escaped protein. Golgi glycosyl transferase and N-acetylglucosaminyl transferase also posses TMDs in their cytoplasmic tails, which are necessary for their retention (20).

Transport intermediates carrying cargo derived from the ER deliver their contents to the *cis* face of the Golgi complex. The cargo molecules then move through stacks of flattened cisternae to the TGN where they are packed into membrane-bound carriers destined for the plasma membrane or for vacuolar storage (28). The two faces of the Golgi complex are functionally different. The *cis* face of the Golgi is the site where pre-Golgi intermediates merge together and the *trans* face would represent older cisternae in the process of segregating and packaging proteins and lipids into post-Golgi transport intermediates (29).

Clathrin-coated vesicles (CCV) are molecules mediating intracellular membrane trafficking such as receptor-mediated endocytosis. In addition to clathrin, the CCV are composed of many other components, including oligomeric adaptor complexes known as clathrin assembly proteins (AP) complexes. The adaptor complexes interact with the cytoplasmic tails of membrane proteins, leading to their selection (12).

Two types of adaptor complexes are known: AP-1 associated with the Golgi complex and AP-2 associated with the plasma membrane. Both AP-1 and AP-2 are heterotetramers consisting of two large chains, the adaptins, (γ and β in AP-1; α and β in AP-2), a medium chain and a small chain. The adaptor proteins AP-1 regulate trafficking of membranes between TGN and endosome/lysosomes through membrane association,

recognition of sorting signals, and recruitment of clathrin and accessory proteins (20, 30).

i. ER-Golgi Protein Cycling

Golgi proteins undergo bidirectional cycling to and from the ER**.** The forward flow of secretory cargo toward the Golgi is balanced by backward flow of selected components to the ER. Golgi cisternae are formed by continuous maturation; that is, by differentiation of pre-Golgi intermediates coupled with the recycling of selected components back to the ER (29). Golgi tubules used in retrograde flow (backward flow from the Golgi to the ER) extend out from the Golgi complex. They are remarkably long and do not detach from the Golgi complex**.** One or more of the tubules fuses with the ER into which the Golgi is then absorbed (26).

The main purpose of the recycling pathway of protein delivery in Golgi is to ensure that resident Golgi enzymes are retained within the system. This was demonstrated by a study in which microtubule disruption prevented peripheral pre-Golgi intermediates from tracking into the Golgi region, and this in turn prevented Golgi proteins from reversibly cycling to and from the ER (31). This result supports the idea that Golgi protein-cycling pathways involve the ER as an intermediate.

Upon reaching the TGN of the Golgi complex, proteins and lipids are packaged into transport intermediates that move through the cytoplasm to fuse with the cell surface or with other storage compartments. Export of anterograde (forward flow from the ER to the Golgi) cargo out of the TGN involves sorting into distinct pathways**.** One of these pathways involves post-Golgi carriers (PGCs), which are large tubular structures, in

addition to small vesicles. They fuse with the plasma membrane without intersecting other membrane pathways in the cell (32).

Not all proteins reaching the Golgi continue within the secretory pathway. In fact some proteins are being retained within the early Golgi cisternae. One of the mechanisms for achieving retention within the Golgi is oligomerization throughout. In this mechanism, Golgi enzymes form oligomers of protein within the compartment, making them too large to enter the anterograde trafficking between different Golgi cisternae and onward to the plasma membranes (12).

MORPHOLOGICAL CHANGES IN THE MEMBRANE SYSTEM DURING DIFFERENT STAGES OF GRAIN DEVELOPMENT

ER structure is present at all stages after fertilization. During the first 1-2 DAA, swollen cisternae of RER are visible. Cisternae also exist at the surface of the dividing nuclei or chromosome mass but they are excluded from the cytoplasmic area that lies between the chromosomes (33).

From 4 to 22 DAA the volume occupied by the RER in the developing endosperm cell increases more than six fold. The large increase in the surface area of RER between 12 and 16 DAA is particularly of great interest. During this time the rate of synthesis and the deposition of storage protein accelerate rapidly. On the other hand, the volume of the smooth ER has a much lower total value than that of the RER throughout the development (33).

PB are typically spherical but their shapes are distorted at maturation due to kernel desiccation and compression by starch granule. Storage proteins start being

developed around 10 DAA in the form of membrane-bound spherical bodies closely associated with RER. Vacuoles are filled at 12-20 DAA and, once they get turgid further deposition, occur within the RER lumen in a process of retention. (33)

EVIDENCE OF DIVERSE EXPRESSION OF CONSTITUTIVE PROTEINS AT DIFFERENT STAGES OF GRAIN DEVELOPMENT

Comparisons were made between immature (17 DAA) and mature (45 DAA) endosperms of *triticum aestivum* to determine changes in protein composition during development. An approximate total of 1298 proteins were expressed at 17 DAA. For endosperm samples at 45 DAA, there were a total of approximately 1125 proteins expressed at this stage of maturity. This led to the suggestion that the number and diversity of proteins in the endosperm change throughout the course of seed maturation, and they are greater at the immature stage (17 DAA) than at maturity (45 DAA). Many of those proteins were either up-regulated or only present at 17 DAA. Some other proteins were down-regulated at 17 DAA or only present at the mature stages. For example, at 17 DAA, when wheat was actively synthesizing proteins, abundant PDI (protein disulfide isomerase) isoforms were present in the endosperm. With the decrease in protein synthesis at 45 DAA, some of the PDI isoforms were no longer expressed in the endosperm (2).

One study showed that both PDI and BiP, which are parts of the machinery that assist in the folding, assembly, and sorting of secretory proteins via the ER, were more abundant in developing endosperm and root tips than in leaves. However, the relative proportions of PDI and BiP varied in different tissues, with PDI being the most abundant

in developing endosperms and BiP being the most abundant in root tips. The expression of both of these proteins in developing endosperms was up-regulated several days prior to the detection of storage proteins. The levels of PDI and BiP declined after 17 DAA (15).

Another class of proteins involved in protein synthesis that is differentially expressed between the two stages of development, 17 and 45 DAA, is the 60S acidic ribosomal proteins. This cluster of proteins is also substantially reduced in the endosperm at 45 DPA in the same manner as PDI (2).

Three wheat cDNA homologues of the ER-resident membrane protein Sec61α (*AtSec61α*), the major subunit of Golgi COPI coatomer COPα (*AtCOPα*), and the plant-specific receptor BP-80 that is localized on Golgi and on prevacuole membranes (*AtBP-80)* were previously isolated. Those three wheat cDNAs encode proteins functioning in different compartments of the endomembrane system. mRNA levels of all three were the highest at the early stages of kernel maturation (8 DAA), and then reduced with the increasing age of the kernels. This is in agreement with the observation that the levels of different endomembrane-associated proteins (BiP, PDI, Sar1, Sec12, calreticulin, and calnexin) are high in young kernels and decreased as the kernel matures (8).

These observations suggest that during the stage of embryo and endosperm differentiation and development, young kernels at the stage of synthesis and accumulation of reserve components possess a highly functional endomembrane system while the maturing kernels have a less active one. Despite the general reduction of the Sec61α, COPα and BP-80 mRNAs levels with kernel maturation, the level of Sec61α mRNA, compared to the other two, is higher in kernels during the stage of storage-protein synthesis relative to young kernels at early stages of maturity(8).

STORAGE-PROTEIN FINAL DISTRIBUTION AND CHARACTERISTICS

Little is known about how storage proteins are organized within PB into their final structure, although this organization may be important in ensuring efficient use of storage space and facilitating mobilization of storage proteins during germination. The separation of different proteins in cereal PB could result from the properties of the proteins themselves, which are embedded in their primary structure, or from different patterns of deposition during PB synthesis.

Mature wheat grains finally contain 8–15% protein, including the gluten storage proteins that are enriched in proline and glutamine. In late stages of development, the abundant gluten proteins constitute up to 80% of total flour protein, and hold properties of elasticity and extensibility that are essential for the functionality of wheat flours (34).

The roles of the individual gluten components in dough functionality are complex. Although high-molecular-weight glutenin subunit proteins (HMW) constitute no more than 10% of total flour protein, they may be the most important determinants of bread-making quality because of their importance in forming the glutenin polymer (35). Generally, albumins and globulins are not thought to play a critical role in flour quality, although the ratio of albumin to globulin was reported to correlate with bread-making quality (36)

LITERATURE CITED

1. Levanony, H., Rubin, R., Altschuler, Y., and Galili, G. 1992. Evidence for a novel route of wheat storage proteins to vacuoles. *J Cell Biol*., 119, 1117-1128.

2. Skylas, D., Mackintosh, J., Cordwell, S., Basseal, D., Walsh, B., Harry, J., Copeland, L., Wrigley, C., and Rathmell, W. 2000. Proteome approach to the characterization of protein composition in the developing and mature wheat-grain endosperm. *J Cer . Sci.,* 32, 169–188.

3. Berger, F. 1999. Endosperm development. *Curr. Opin. Plant Biol.,* 2, 28–32.

4. Lohe, A., and Chaudhury, A. 2002. Genetic and epigenetic processes in seed development. *Cur. Opin. Plant Biol.,* 5, 19–25.

5. Sofield, I. Evans, L., Cook, M., and Wardlaw, I. 1977. Factors influencing the rate and duration of grain filling in wheat. *Aust. J. Plant Physiol.,* 4: 785–797.

6. Young, T. and Gallie, D. 1999. Analysis of programmed cell death in wheat endosperm reveals differences in endosperm development between cereals. *Plant Mol. Biol.,* 39, 915–926.

7. Olsen, O. 2001. Endosperm development: cellularization and cell fate specification. *Ann. Rev. Plant Biol.,* 52, 233–267.

8. Feeney, K., Tatham, A., Gilbert, S., Fido, R., Halford, N., and Shewry, P. 2001. Synthesis, expression and characterization of peptides comprised of perfect repeat motifs based on a wheat seed storage protein. *Bioch. Biophys. Acta,* 1546, 346-355.

9. Shewry, P., Napier, J., and Tatham, A.1995. Seed storage proteins: structures and biosynthesis. *Plant Cell*., 7, 945-956.

10. White, S., and Wimley, W. 1999. Membrane protein folding and stability: physical principles. *Annu. Rev. Biophys. Biomol. Struct*., 28, 319–365.

11. Meacock, S., Lecomte, F., Crawshaw, S., and High, S. 2002. Different transmembrane domains associate with distinct endoplasmic reticulum components during membrane integration of a polytopic protein. *Mol.Biol. Cell* 13, 4114-4129.

12. Lippincott-Schwartz, J., Roberts, T., and Hirschberg, K. 2000. Secretory protein trafficking and organelle dynamics in living cells. *Ann. Rev. Cell Develop., Biol.* 16, 557-589.

13. Dayel, M., Hom, E., and Verkman, A. 1999. Diffusion of green fluorescent protein in the aqueous-phase lumen of endoplasmic reticulum. *Biophys. J,* 76, 2843-2851.

14. Nehls, S., Snapp, E., Cole, N., Zaal, K., and Kenworthy, A. 2000. Dynamics and retention of misfolded proteins in native ER membranes. *Nat. Cell Biol.,* 2, 288-295.

15. Roden, L., Miflin, B., and Freedman, R. 1982. Protein disulphide isomerase is located in the endoplasmic reticulum of developing wheat endosperm. *FEBS ,* 138, 121-124.

16. Shimoni, Y., Zhu, X., Levanony, H., Segal, G., and Galili, G. 1995. Purification, characterization, and intracellular localization of clycosylated protein disulfide isomerase from wheat grains. *Plant Physiol.,* 108, 327-335.

17. Bechtel, D., Gaines, R., and Pomeranz, Y. 1982. Early stages in wheat endosperm formation and protein body initiation. *Ann. Bot.,* 50, 507-518.

18. Larkin, B., and Hurkman ,W., 1978. Synthesis and deposition of zein in protein bodies of maize endosperm. *Plant Physiol.,* 62, 256-263.

19. Hermo, L., and Smith, C. 1998. The structure of the Golgi apparatus: a sperm's eye view in principal epithelial cells of the rat epididymis. *Histochem .J Cell Biol.,* 109, 431-447.

20. Gomord, V., Wee, E., and Faye, L. 1999. Protein Retention and Localization in the Endoplasmic Reticulum and Golgi apparatus. *Biochimie*., 81, 607-618.

21. Hammond, C., and Helenius, A. 1995. Quality control in the secretory pathway. *Curr. Opin. Cell Biol.* 7, 523-529.

22. Kuge, O., Dascher, C., Orci, L., Rowe, T., Amherdt, M. 1994. Sar1 promotes vesicle budding from the endoplasmic reticulum but not Golgi compartments. *J Cell Biol.,* 125, 51-65.

23. Hammond, A., and Glick, B. 2000. Dynamics of transitional endoplasmic reticulum sites in vertebrate cells. *Mol. Biol. Cell* 11, 3013-3030.

24. Klumperman, J., Schweizer, A., Clausen, H., Tang, B., and Hong, W. 1998. The recycling pathway of protein ERGIC-53 and dynamics of the ER-Golgi intermediate compartment. *J Cell Sci.,* 111, 3411-3425.

25. Lippincott-Schwartz, J., Cole, N., and Donaldson, J. 1998. Building a secretory apparatus: role of ARF1/COPI in Golgi biogenesis and maintenance. *Histochem. Cell Biol.,* 109, 449-462.

26. Sciaky, N., Presley, J., Smith, C., Zaal, K., and Cole, N. 1997. Golgi tubule traffic and the effects of brefeldin A visualized in living cells. *Cell Biol.,* 139, 1137-1155.

27. Mollenhauer, H., and Morre, D. 1994. Structure of Golgi apparatus. *Protoplasma*. 180, 14-28.

28. Polishuk, R. and Mironov, A. 2004. Structural aspect of Golgi function. *Cell Mol. Life Sci.*, 61, 146-158.

29-Pelham, H. 1998. Getting through the Golgi complex. *Trends Cell Biol.* 8:45-49.

30-Chou, K. and Elrod, D. 1999. Protein subcellular location prediction. *Prot. Eng*. 12: 107–118.

31-Zaal, K., Smith, C., Polishchuk, R., Altan, N., and Cole, N. 1999. Golgi membranes are absorbed into and reemerge from the ER during mitosis. *Cell* 99:589-601.

32-Kreitzer, G., Marmorstein, A., Okamoto, P., Vallee R. and Rodriguez-Boulan, E. 2000. Kinesin and dynamin are required for post-Golgi transport of a plasma-membrane protein. *Nat. Cell Biol.* 2:125-27.

33-Simmonds, D. and O'Brien, T. 1981. Morphological and Biochemical Development of the Wheat Endosperm. In: *Advances in Cereal Science and Technology*. Ed: Pomeranze Y. St. Paul, Minnesota. pp: 27-46.

34-Shewry, P., Tatham, A., Barcelo, B., and Lazzeri, P. 1995. Biotechnology of breadmaking: unraveling and manipulating the multi-protein gluten complex. *Biotechnology* 13: 1185–1190.

35-Gupta, R., Batey, I. and MacRitchie F. 1992. Relationships between protein composition and functional properties of wheat flours. *J. Cer.Chem.* 69: 125–131.

36-Pence, J., Weinstein, N. and Mecham D. 1954. The albumin and globulin contents of wheat flour and their relationship to protein quality. *J. Cer. Chem.* 31: 303–311.

CHAPTER II

A METHOD OF ENRICHMENT OF THE ENDOPLASMIC RETICULUM AND GOLGI COMPLEX PROTEINS FROM WHEAT SEEDS (*TRITICUM AESTIVUM*) AT DIFFERENT STAGES OF GROWTH

INTRODUCTION

In bread making, bread-wheat (*Triticum aestivum*) protein quality and content are recognized as major factors in distinguishing the functional properties of different wheat cultivars (1). During wheat-seed development, there is a shift from a state of cell division to a state of grain filling. Some of the most important factors in determining the final protein content of seeds are timing, duration and rate of grain filling; all of these would affect the end-product performance of wheat. It is widely known that those factors are affected by the growth conditions (2).

Wheat end-product diversity continues to increase on a daily basis in household use and in industrial applications. The latter demands a greater attention to wheat quality and its performance during highly mechanized processing. There is a need to understand the relationship of genetics to processing quality in wheat. Understanding this relationship under optimum conditions will assist in obtaining the baseline of the factors contributing to wheat quality. As the first product of gene activity, proteomics are critical to understanding the gene-function relationship and the effects of storage protein quality on processing quality (3).

Identification of individual proteins as markers of phenotypes has a great impact on improving wheat production, from breeding to quality testing in bread production. The subcellular system involved in protein synthesis is suspected to be a determinant of the processing and nutritional value of wheat endosperm. In this context, the importance of the endoplasmic reticulum (ER) and the Golgi complex (GC) as major determinants of the metabolic fate in seed plants is speculated, due to their involvement in protein processing and posttranslational modification. Because wheat endosperm displays a shift

from the state of cellular division to a state of grain filling, the function of the ER and GC is speculated to show functional diversity during different stages of wheat development. However, studies of the diversity of protein composition in these organelles during different stages of wheat growth are still missing. An important feature would be a descriptive study of the constitutive proteins of these organelles at different stages of development. This descriptive study could be used to build a comparative database of the organelles' protein expression at different stages of growth.

Subcellular protein fractions of the secretory pathways, particularly the ER and GC, are known for their active protein trafficking from the cytosol and for their involvement in many regulatory pathways as signaling, targeting and processing. The ER is known for its protein folding, assembly, degradation and transport. Secretory cargo is cotranslationally synthesized and assembled in the ER and then, depending on the wheat growth stage, secreted proteins may either reside locally or leave the ER via distinct exit sites that bud and translocate as tubulovesicular structures (pre-Golgi) toward the microtubules. At this point, the destination is to merge with Golgi membranes for further processing and maturation. Upon arrival at the *trans*-Golgi network (TGN) which is the distal Golgi part, proteins are sorted and packaged into post-Golgi carriers that move through the cytoplasm in microtubules to reside in storage vacuoles or to fuse with the cell surface (4).

Those regulatory pathways would eventually determine the storage protein composition and content in seeds. Constitutive proteins from the ER and GC are suspected to show a diverse expression at different stages of growth. Seven days after anthesis (DAA) represents the early stage of wheat endosperm development. This is the

stage where the plant starts actively synthesizing storage proteins. The complexity of the membrane protein development is expected to increase as the storage protein synthesis begins, which is approximately around 14 DAA, and then to start declining around 34 DAA, representing the end of storage protein synthesis. Some reports suggested that a wider profile of constitutive proteins exists at immature stages where protein manufacturing is at its maximum, compared to mature stages (5). However, little information is available on how those proteins are developed. Through monitoring the constitutive protein expressions in the ER and GC, it may be possible to identify the presence or absence of individual proteins undergoing expression at each developmental stage.

The objective of this project was to optimize a fractionation method to allow identification the proteomic profile of the two organelles, the ER and the GC from wheat endosperm. Our hypothesis is that the constitutive proteins of these organelles in wheat seeds show a qualitative diversity in expression at early, middle and late stages of growth under optimum growth conditions. The information reported from the expression of the individual proteins will be collected in a descriptive study. The study can be used in future work to generate a comparative database of the organelles' protein expression and at different developmental stages in an attempt to identify their individual roles as phenotypes markers.

The optimized methodology used in fractionating and identifying the constitutive proteins includes discontinuous sucrose gradient fractionation to separate the membranes of the ER and GC on a crude basis, followed by a partitioning with an aqueous two-phase system to increase the separation obtained from fractionation. The two-phase partitioning

procedure reduced contamination by separating organelles from plastids in suspension according to their partition coefficient. 1-D Sodium Dodecyl Sulfate-Polyacrylamide Gel Electrophoresis (SDS-PAGE) revealed the pattern of fractionation and enrichment of different fractions. 2-D electrophoresis resolved complex bands according to their Isoelectric Focusing point (IEF) in the first dimension and to their apparent molecular size in the second dimension. Finally Matrix Assisted Laser Desorption Ionization-Time of Flight (MALDT-TOF) was used to determine the identity of the selected proteins by peptide mass fingerprinting and MS-FIT search. Eventually, the completion of such a comparative database would allow speculation on the identified proteins' possible effect on seed growth and grain filling.

MATERIALS AND METHODS

Procedure for Wheat Seed Growth

Wheat plants were grown at the Oklahoma State University greenhouse facilities. The seeds for *Triticum aestivum* (Butte 86) were sterilized for 30 seconds in 1% silver nitrate ($AgNO_3$) in a sonicator and washed three times for 5 min in MilliQ ultrapure water with continuous stirring. Seedlings were planted at a depth of 1 cm in 1-gallon pots containing Metro-Mix 666 soil brand. A Miracle Grow® brand fertilizer was added once per week as instructed by the manufacturer (1 full cup for 3 gallons of water). Plants were grown at a rate of 4 seeds per pot in batches of 480 pots. Each spike was tagged with the date of anthesis.

Growth Curve: Weight of Seeds Vs. Time

The growth curve representing fresh and dry weight of wheat seeds as a function of time (DAA) is presented in Figure 1. The points on the curve are averages of three independent observations consisting of three spikes containing a range of 23 to 32 seeds. Pots were randomly selected and spikes harvested at 7, 14, 34 and 60 (DAA). The specific number of seeds per spike was recorded. Fresh weight of seeds was recorded then the seeds were freeze dried and their dry weight recorded.

Fractionation of the ER and GC

The method of fractionation of the ER and GC wheat endosperm is a modification of the method of Morre et al for green leaves (6, 7). All procedures were conducted at 4°C. A sample of approximately 200 g of dry wheat was collected and dehulled using a

Seeburo barely pearler (Seedburo Equipment Co, Chicago, IL). The pearler was equipped with a 30 grit carborundum stone and a No. 7 mesh screen. Pearling was conducted until the brownish mature seeds turned shiny white to ensure a complete removal of the pericarp outer layer. This will remove about 1/3 of the seeds' weight. The pearling step is necessary to remove any coating pericarp not pertaining to the endosperm, which eventually helps reduce contamination. Pearled seeds were next ground using a Lafret grinder (Brabender Instrument Inc, Hackensack, NJ) at the scale setting number 1. This setting gives a particle size of 1-2 mm in diameter.

The extraction buffer consisted of 50 mM HEPES ($C_8H_{18}N_2O_4S$), 10 mM KCl, 1 mM EDTA ($C_{10}H_{16}N_2O_8$), 10 mM ascorbate ($C_6H_8O_6$), 5 mM DTT (dithiothreitol: $C_4H_{10}O_2S_2$) and 0.4 M sucrose at a pH of 7.4. Bovine serum albumin was omitted from the original method (6, 7) due to its masking effect on the proteomics profile, and replaced with 15 mM CsCl to preserve the osmotic effect of the solution. The buffer was pre-cooled at 4°C for 2-3 hours with continuous stirring, and 5 min before use, mixed with Complete Protease Inhibitor Cocktail tablets (Roche) at a ratio of 1 tablet for every 50 ml of buffer solution.

For mature wheat, the buffer was added to the wheat at a 1:3 ratio (w/v), and ground in a chilled mortar and pestle. The grinding procedure was conducted for 15-20 min in an ice bath and the homogenate filtered through four layers of cheesecloth. The filtrate was centrifuged for 10 min at 1000 x g at 4°C in an SS-34 fixed angle Sorval rotor (Sorvall Kendro, Asheville, NC). The supernatant was immediately used in the following steps or frozen in liquid nitrogen using cryogenic vials and stored at -80°C for later use.

250 g of seeds coming from earlier stages of development were squeezed to collect a pasty white-yellowish endosperm, stored in cryogenic vials, immersed immediately in liquid nitrogen and frozen at -80°C for later use. At the time of use, the buffer was added to the endosperm samples at a ratio of 1:2 (w/v).

Using 35 ml tubes, a 15 ml aliquot of supernatant, instead of 10 ml as reported in the method of Morre et al. (6), was layered onto discontinuous sucrose gradients consisting of 6 ml 37% and 10 ml 21.5% (w/v) sucrose instead of 4 and 6 ml respectively. The concentration of the sucrose solutions was adjusted using a refractometer Leica AutoAbbe (Leica Inc., Buffalo, NY). The layered preparations were centrifuged using a Beckman swing SW-28 rotor at 4°C (Beckman-Coulter, Fullerton, CA) for 30 min at 22,000 rpm (65,000 x g). The interphase at the homogenate/21.5% layers contained the ER in a crude form whereas the interphase at the 21.5 - 37% contained the GC in a crude form.

Crude ER and GC fractions were collected in separate tubes using a Pasteur long-neck transfer glass pipette. In order to remove the sucrose, the fractions were diluted with the same extraction buffer solution without sucrose and layered on top of a 1.6 M sucrose cushion. The layers were centrifuged for 20 min at 20,000 rpm (53,000 x g) using a swing rotor Beckman SW-28 at 4°C and the ER and GC extracts were collected at the interphases. The addition of the 1.6 M sucrose layer at the bottom of the centrifuge tube led to the collection of fractions at the cushion interphase. This step is a modification of the original method intended to keep the fractions out of pelleting and aggregation. This in turn provides a better solubilization needed in the two-phase partitioning rather than pelleting, as suggested by Morre et al (6).

Two-phase Partitioning

The two-phase partitioning separates substances according to their partition coefficient, which in turn depends on several factors, including surface charge of the partitioned membranes, density, pH range, buffer and polymer concentrations. All of these factors vary among separated material. To remove contaminating plastids the pellets were resuspended in phosphate buffer at a concentration of 100-150 mg/ml. The phosphate buffer consisted of 2 ml of 0.25 M sucrose containing 5mM potassium phosphate (HK_2O_4P), pH 6.8.

In the method of Morre et al (7) designed for partitioning of spinach-leaf organelles, the resuspended crude organelle fractions were applied to a 5.9% (w/w) two-phase partitioning system consisting of Dextran (DEX) T-500 with polyethylene glycol 4000 (PEG). By the addition of water the total system was brought up to a 16 g total. However, by applying this method in wheat endosperm fractions, a substantial precipitation of a green-yellowish precipitate was obtained.

A series of polymer dilutions were assayed to eliminate this precipitation, ranging from 5.0 to 6.5% of polymers with an increment of 0.1% at a time. The optimum polymer concentration that decreased precipitation to a minimum was at 5.6%. The total weight of the mixture was kept at 16 g for every 100-150 mg of protein applied.

Tubes were inverted 40 times and centrifuged at low speed in an SS-34 fixed-angle Sorval rotor (7 min at 1000 x g) at 4°C to obtain two layers. The upper layer, along with the interphase, both containing plastids, were removed using a Pasteur long-neck transfer glass pipette, leaving the lower layer in the separation tube. The obtained lower layer was diluted about 10 times with the extraction buffer without sucrose and

centrifuged at 20,000 rpm (53,000 x g) for 20 min at 4ºC to yield a pellet containing enriched fractions of organelles (ER and GC).

Separation of Smooth and Rough ER

Separation of smooth and rough ER was adopted from the method of Bergstrand et al (8). Briefly, 3 ml of 1.3 M sucrose and 1.5 ml of 0.6 M sucrose were respectively layered in a centrifuge tube. The ER pellet was resuspended in 0.25 M sucrose solution, to which CsCl was added to obtain a final concentration of 15 mM. The solution was layered on top of the sucrose layers to the maximum capacity of the tube and centrifuged at 25,000 rpm (82,700 x g) for 132 min at 4 ºC using an SW 28 rotor. The smooth ER fraction was collected from the 0.6-1.3 M interphase and the rough ER from the pellet.

Ribosome Stripping from Rough ER

Puromycin was used for stripping ribosomes from the enriched rough ER fractions of wheat endosperms. A modified method of Kreibich et al (9) was developed. The rough ER fractions were resuspended in 2 ml of low salt buffer consisting of 50 mM KCl, 50 mM Tris-HCl pH 7.5, and 5 mM $MgCl_2$. The final ion concentration was adjusted with a compensating buffer to high-salt buffer A consisting of 500 mM KCl, 50 mM Tris-HCl pH 7.5, and 2.5 mM $MgCl_2$. Puromycin at a concentration of $1x10^{-3}$ M was added. The suspension was incubated for 20 min at 20°C and for 10 min at 37°C.

The suspensions were diluted 4 times with high-salt buffer B, consisting of 500 mM KCl, 50 mM Tris-HCl pH 7.5, and 5 mM $MgCl_2$. The fractions stripped of ribosomes were recovered by sedimentation for 30 min at 40,000 rpm at 4 ºC using a rotor Beckman 45Ti using a sucrose cushion consisting of 4 ml of 20% sucrose and high-salt buffer B.

Quantitative Protein Determination by BCA

Protein content of all fractions was determined using a bicinchoninic acid (BCA) kit from Sigma-Aldrich (St. Louis, MO). The BCA complex was prepared by mixing 50 parts of bicinchoninic acid to 1 part of copper II sulfate pentahydrate. All protein fractions were added to the complex at 1% (v/v) and heated at 60 °C for 15 min. To prepare a standard calibration curve, a series of bovine-serum albumin (BSA) dilutions at 1, 0.8, 0.6, 0.4 and 0.2 mg/ml were prepared and added to the complex at a ratio of 1%. The absorbance was recorded at 562 nm.

SDS-PAGE

The patterns of fractionation and enrichment were monitored by 1-D SDS-PAGE. The fractions designated crude extract represent the fraction obtained after the low-speed centrifugation at 1000 x g. The fractions-designated crude organelles (both ER and GC) represent the fractions obtained after the separation with the discontinuous sucrose gradient. The fractions-designated enriched organelles represent the fractions obtained after ribosome removal of the rough ER and after the two-phase partitioning for the GC. Gels were made of 12% acrylamide and 1% bis-acrylamide (cross linker). Gels were run

at 20 mA for 10 hours and developed using 0.5% (w/v) Comassie blue, 50% (v/v) methanol and 10% acetic acid. Gels were later destained overnight using 25% methanol and 10% acetic acid. A 100 µl of each fraction was loaded in every well.

Immunodetection of the ER and GC Enzyme Markers

To test for the enrichment of the ER and GC during the fractionation steps, Western blot analysis was performed using PVDF transfer membrane and alkaline phosphatase for the rapid immunodetection (chromogenic) of enzyme markers. Protein transfer was conducted for 1 hour at 100 V. Alkaline phosphatase was the label for the second antibody, developed using BCIP/NBT as substrates, to yield an intense purple-black color on the target bands.

The enzyme markers used in blotting were calreticulin (CRT) for the ER and formiminotransferase cyclodeaminase (FTCD) for the GC. CRT is a 46 kDa protein serving as a molecular chaperone in the ER of eukaryotic cells. It is involved in Ca^{2+} storage and intracellular Ca^{2+} signaling in the ER (10). FTCD is a 58 kDa enzyme associated with the cytoplasmic surface of the GC. It is a bifunctional enzyme that catalyzes two consecutive steps in the modification of tetrahydrofolate to 5,10-methenyl tetrahydrofolate (11). Anticalreticulin rabbit antiserra (Novus Biological, Littleton, CO) was used as primary antibody and goat polyclonal anti-rabbit (Abcam, Cambridge, UK) as a secondary antibody for the ER enzyme marker. For the GC marker, mouse monoclonal to FTCD (Abcam, Cambridge, UK) was the primary antibody and rabbit polyclonal to mouse (Abcam, Cambridge, UK) was the secondary antibody marker for the GC.

2-D Electrophoresis

Proteins were resolved by 2-D electrophoresis according to the method of Skylas et al (12). 30 µg of pellets of enriched organelles were resuspended in 300 µl of solubilization buffer consisting of 7 M urea, 2 M thiourea, 2 mM tributyl phosphine (TBP), 4% 3-[(3-cholamidopropyl) dimethylammonio]-1-propane sulphonate (CHAPS), 2 % carrier ampholytes (3-10 Biolytes, Amersham Pharmacia Biotech, Sweden), 40 mM Tris, bromophenol blue dye and MilliQ water to make up the volume.

Samples were vortexed for 30 sec then centrifuged for 1 min at 13,200 rpm at room temperature, and the supernatant was collected. An aliquot of 250 µl of supernatant was applied to the strip holder and covered with analytical Immobilised pH Gradient strips (IPG, 13 cm) pH 3.0–10.0 (Amersham Pharmacia Biotech, Sweden) and covered with DryStrip Cover Fluid (Biotech AB, Uppsala Sweden). Strips were rehydrated overnight and IEF was performed using an IPGphore system (Pharmacia Biotech, Sweden) in a step-wise protocol with 500 V in step 1 (1 hr), 1000 V in step 2 (1 hr) and 8000 V in step 3 (2 hr). IPG strips were equilibrated in buffer consisting of 6 M urea, 2% SDS, 50 mM Tris/HCl pH 8.8, 30% glycerol, and 0.002% bromophenol blue and water to make up the volume.

To 10 ml of this buffer, 100 mg DTT were added as a reducing agent. The buffer was applied to the strips and washed for 15 min. A second equilibration was applied with the addition of 250 mg iodoacetamide (IAA, ICH_2CONH_2) as an alkylating agent and the strips were washed for 15 min and then mounted on SDS-PAGE gels 12% acrylamide, using a strip-fixing solution consisting of 0.5% agarose in SDS-electrophoresis running buffer and 0.0002% (w/v) bromophenol bleu. Gels were run as described earlier in the 1-

D SDS-PAGE. A Bio-Rad silver staining kit (Bio-Rad Laboratories Inc., USA) was used for gel silver staining.

Peptide Mass Fingerprinting Using MALDI-TOF

The procedure for in-gel digestion of protein spots excised from silver-stained gels was performed using a modification of the method described by Shevchenko et al (13) and used by the Recombinant DNA/Protein Resource Facility. Preliminary testing confirmed no significant difference in spectrum intensity between silver-stained and destained gels. Therefore, gels were used without destaining. Negative control slices from empty regions of the gel were selected. Briefly, gel plugs were excised from gel using disposable cocktail straws pre-soaked with ethanol 70% for 1 min and air dried. Gel plugs were soaked twice, 1 hr each with 50% acetonitrile (ACN) mixed with 0.1% trifluoroacetic acid (TFA). Plugs were later soaked overnight with high-purity water (EM Science, Darmstadt, Germany). The next day, the plugs were dehydrated completely with 100% ACN and reduced using 0.15% DTT in 0.2% ammonium bicarbonate ($(NH_4)_2CO_3$, Sigma, St. Louis, Missouri) at 56 ºC for 1 hr. The plugs were next alkylated using 0.2% IAA in 0.2% ammonium bicarbonate at room temperature for 1 hr. Later, the plugs were rinsed with 0.2% ammonium bicarbonate and dehydrated with 100% ACN. A 20 µl sequencing grade-modified trypsin solution (Promega, Madison, WI), was used at a concentration of 8.3 µg/ml at 37 ºC for 4 hr. Peptides were extracted three times by incubating with 20µl of 0.1% TFA for 2 hr each.

Protein identification was carried on at the Recombinant DNA/Protein Resource Facility, Department of Biochemistry and Molecular Biology at Oklahoma State

University. Peptide mass fingerprints were analyzed using the autosequencing program of MALDI-TOF (Voyager DE-PRO mass spectrometer, Framingham, MA). The spectrum acquisition limits were set at maximum number of 50, and the detected mass range at 700-3000 kDa. The operating mode was set at the reflector and the laser intensity 2,200. Spectrum acceptance criteria were set at signal intensity 5,000 minimum and 50,000 maximum. The criteria evaluation mass range was 1,100-2,400 and the spectrum accumulation was 5.

RESULTS

Weight Change of Wheat Seeds versus Time

The change of fresh and dry weight of endosperm wheat during the grain filling stages (growth curve) is presented in Figure 1. Observations were recorded at 4 time-points: 7, 14, 34, and 60 DAA. Each point represents an average seed weight of three full wheat heads made on three different observations. Dry weight was obtained from freeze-dried seeds. The growth curve suggests a fast weight accumulation rate up to 14 DAA followed by a plateau (fresh weight) or a slower rate of weight of accumulation (dry weight). These observations are in agreement with previous studies (5, 14). During the grain-filling stage proteins and carbohydrates are synthesized, resulting in the endosperm development. During the early grain filling stages the endosperm is in a milky stage with high moisture content. As the grain filling advances (14 to 34 DAA), the moisture content decreases and the total solids (protein, carbohydrate, lipids and other minor components) increase. Figure 1 suggests that water accumulation is about 2 times the accumulation of solids during the period between 7 and 14 DAA. The period between 34 and 60 DAA is considered a maturation period when desiccation of the seeds take place. As the moisture content is reduced, the cell and organelle membranes collapse.

Protein Recovery

The enrichment of organelles from wheat endosperm is represented in Table 1. Enrichment rates are presented as concentration, percentage of recovery changes and fold reduction of protein content through enrichment stages. At 7 DAA, about 80% and 88 % of the crude extract protein content were eliminated by the sucrose gradient fractionation

to obtain crude ER and GC. This elimination consists mainly of storage, nuclear, and mitochondrial proteins (7). The two-phase partitioning, the second step of the enrichment, removed a large fraction of plastid fragments from both crude ER and GC yielding about 2% of enriched ER and 1% of enriched GC fraction from the original crude extract.

In mature wheat, the protein recovered from the crude extract by the sucrose gradient fractionation of the ER and GC was 19.1% and 12% respectively. The two-phase partitioning and further treatment recovered 1.85% of En ER and 1% of En GC by the removal of a major portion of plastids contamination.

Both enriched fractions of 14 and 34 DAA appeared to have the highest percentage of protein recovery after fractionation to obtain enriched ER and GC fractions (4.7 and 4.2% for ER and 1.7 and 1.6% for GC respectively). The percentage of protein recovered at the enriched 7 DAA is higher than the 60 DAA. However, the 34 DAA showed a lower percentage of recovered protein than the 14 DAA due to a higher of loss of protein during fractionation and enrichment.

The fractionation of the crude extract to En ER and En GC at 7 DAA resulted in a reduction of protein concentration of about 530 times and 100 times respectively. In the 14 DAA En ER and En GC fractions, about 20 and 60 times of the crude extract were reduced. About 25 and 65 times of the crude extract were reduced in obtaining the En ER and En GC at 34 DAA, and about 95 and 160 times in obtaining the enriched 60 DAA fractions. The 34 DAA is slightly the highest protein concentration obtained in the ER fractions (4.2 mg/ml). The 34 DAA fraction is higher in concentration than the 14 DAA (1.6 and 1.4 mg/ml), despite that it was lower than the 14 DAA in recovery rate.

Protein Patterns from the Enrichment Steps

The protein pattern from the enrichment of the ER and GC of wheat endosperm extract during the grain-filling stages is reported in Figure 2 (1-D SDS-PAGE). Aliquots of 100 µl from different extracts of endosperm sample were loaded on each well.

The crude extract (Cr EX) represents the fraction obtained by a low-speed centrifugation at 1000 x g which removed debris and unbroken cells. This fraction still includes nuclear, mitochondrial and tonoplasts extracts. Crude fractions for both the ER (Cr ER) and Golgi (Cr GC), obtained by sucrose gradient separation at 22,000 rpm (65,000 x g), show a pattern of band elimination and enrichment. The enriched fractions of organelles, obtained by a two-phase aqueous partition and further treatments, also show a removal pattern of plastids proteins and other contaminants as well as some appearance of new bands. The enriched fractions represent the final steps in the fractionation procedures where a large portion of plastids were eliminated.

Comparison of ER and GC Similarity

The following observations were concluded from the SDS-PAGE results and protein determination (BCA method). The enrichment trend shows qualitative changes in the protein profile among various bands.

The 7 DAA enriched ER and GC fractions show similarity of protein below 60 kDa. Proteins around 90 kDa were eliminated from both fractions compared to the crude fractions. At 14 DAA the similarity of protein pattern is also appearing below 60 kDa in the enriched fractions. By comparison to the crude fractions of the ER and GC, protein below 30 kDa appeared to be absent at the concentration level assayed in the gel. At 34 DAA, the pattern of proteins also shows some similarity below 37 kDa of the enriched

fractions except for one band at 20 kDa in the En GC, probably due to a trend of protein differentiation. The difference between the ER and GC appears to be in the higher molecular weight proteins (above 70 kDa). The elimination of bands between 100-150 kDa from crude ER and GC at 34 DAA is unique to this stage of growth. A differentiation in the functions of the ER and GC and a homogenization-induced fragmentation are possible reasons in the difference in protein pattern between the GC and ER at both levels. The mature (60 DAA) ER and GC fractions at the enriched level show differences in the upper molecular weight range (90-110 kDa) despite the fact that that the endosperm physiology has stopped at this stage of maturity. This showing differentiation is less than the one seen at 34 DAA. The protein profile at this stage is significantly different from the immature stages with a group of dense low molecular weight peptide bands appearing appeared below 12 kDa. This is probably due to fragmentation of many peptides resulting from the desiccation of endosperm at this stage of growth.

In summary, both fractions of the ER and GC show some similarity of the enriched samples in the polypeptide molecular weight range of 30-60 kDa present in all stages. The highest differentiation in protein patterns among all enriched fractions of the ER and GC was observed at 34 DAA, possibly due to the effect of homogenization-induced fragmentation or to the functional diversity occurring at the full maturity of the organelles.

Comparison of the Sucrose Gradient Fractionation Steps

Fractions showed a decrease in protein concentration proportional to the fractionation step (Table 1). At 7 DAA the sucrose gradient fractionation from the crude

extract (Cr EX) to yield crude ER and GC (Cr ER and GC) resulted in 5.2 and 8.3 times reduction in protein content (Table 1). Overall, the protein patterns of the Cr ER and Cr GC fractions appeared to be similar, except for a band around 90 kDa in the Cr GC that is not present in the Cr ER (Fig. 2). The GC appears to have a low concentration or no band lower than 30 kDa. A difference in protein concentration between Cr EX and Crude organelle fractions cannot be observed in the SDS-PAGE. At 14 DAA reduction of protein pattern is appearing in the SDS-PAGE for both the crude organelle fractions compared to the crude extract fraction. The sucrose gradient reduced the protein concentration of the Cr ER and Cr GC by 4.4 and 6.7 times respectively, compared to the crude extract (Table 1). Fig. 2 suggests the appearance of a band at 70 kDa and the elimination of bands between 60 and 37 kDa and below 20 kDa. However, similar to the 7 DAA, the reduction on protein concentration between the crude extract and the crude organelle fraction cannot be concluded from the SDS-PAGE. At 34 DAA, the reduction of protein concentration after sucrose gradient fractionation was 3.5 and 5.3 times for the Cr ER and Cr GC respectively (Table 1). Some bands eliminated from the GC are in range of 15 to 20 kDa. At 60 DAA, the protein concentration reduction following the sucrose gradient was 4.8 and 6.4 times for crude fractions of the ER and GC (Table 1). The fractionation to yield Cr ER from Cr EX led to less enrichment of bands (limited to bands between 60 and 70 kDa) compared to the 34 DAA, possibly due to the process of fragmentation. Samples for SDS-PAGE were loaded on equal volume of extract per well, coming from a starting sample of about 200 g, and not equal protein per well. The lightness of bands in the enriched fractions possibly represents lower protein concentration or a limited solubility of proteins.

Except for the En 60 DAA, the reduction in the protein pattern and concentration of the enriched fractions compared to the Cr EX is appearing on the SDS-PAGE. All immature fractions show a nearly complete absence of the low molecular weight protein bands. A 20 kDa band in the En GC fraction at 34 DAA is an exception. Though a difference in protein concentration between both enriched fractions of 7 DAA was not observed in the SDS-PAGE, both fractions show reductions in the protein patterns compared to the Cr EX. The protein concentration of both enriched fraction is probably too low to show a difference. At both 14 and 34 DAA, the En ER fraction was 3 times the concentration of the En GC fraction. Also these results cannot be observed in the SDS-PAGE. For the 60 DAA, the En ER has more protein than the GC, which agrees with the concentrations reported by the BCA for these fractions. In conclusion, organelle fractions show a decrease in protein content proportional to the stage of fractionation. These results are concluded from the protein concentration assay and from the SDS-PAGE. The ractionation step from crude extract to crude organelles (ER or GC) is observed in SDS-PAGE in the form of band elimination rather than reduction in protein concentration. The fractionation step yielding enriched fractions is seen by elimination of bands as well as by reduction of protein concentration.

Comparison of the Same Organelle across Time

Samples collected at 7 DAA and 14 DAA seem to have similar patterns of protein at the Cr EX fraction, with the 14 DAA fraction having more bands between 75 and 100 kDa. At 34 DAA, the crude extract fraction has the largest protein pattern where the first major band is around 130 kDa. The Cr EX of 60 DAA has the smallest protein pattern among all Cr EXes. The first major band is around 65 kDa and a number of bands of low

molecular weight (10-15 kDa) are present, possibly due to peptide fragmentation. It is postulated that at the mature stage, fragmentation due to collapsing membranes and other cell structures may induce peptide hydrolysis. The higher total protein of the crude extract (113 mg/ml, Table 1) may be in the form of mostly small peptides, compared to the extracts at earlier developmental stages. All the extracts at 60 DAA showed higher number and intensity of bands at and below 15 kDa.

At 7 DAA the Cr ER suggests fewer bands than the 14 DAA fraction. The 14 DAA fraction in turn suggests fewer bands than the 34 DAA. The fractions of 14 and 34 DAA show more similarity compared to the other fractions, except that the 34 has more bands at 120 and 130 kDa. The 60 DAA fraction has less intense bands than both the14 and 34 DAA but still has more intense bands than the 7 DAA. The Cr GC protein pattern is the largest pattern in the 34 DAA fraction followed by 14 DAA and the 60 DAA.

The 34 DAA En ER fraction is more concentrated than all of the fractions. The 60 DAA fraction comes next in protein concentration followed by the 14 and the 7 DAA fraction. The band concentration of the En GC fraction is lower in the 7 DAA fraction than in the 14 DAA. Similar to the En ER fraction pattern, the fraction of the 34 DAA En GC is more concentrated than that of the 14 DAA.

It is concluded that except for the crude extract, all other fractions show an increasing trend of protein concentration relative to the mature stage, with the 34 DAA fraction being the highest concentration.

Western Blot for Enzyme Markers of Organelles

The immunodetection of the enriched fractions of organelles through Western blot using a primary antibody against CRT in the ER revealed a band blotting around 46 kDa, corresponding to the molecular size of CRT (Fig. 3). However, the primary antibody cross-reacted with a low-molecular-weight peptide in all the ER fractions. This antibody was not reported to be tested in plant tissues (http://www.novus-biologicals.com/data_sheet.php/4/S/calreticulin/0). In the GC fraction this antibody tested faintly positive, indicating a minor contamination of the GC fraction with ER. On the other hand, testing the GC fraction with a primary antibody against the FTCD revealed a band at 58 kDa corresponding to the molecular size of FTCD. Testing the same antibody against the ER fraction didn't reveal any blotting reaction.

Descriptive Analysis of Enriched Organelles Proteins Visualized by the 2-D Elecrophoresis and **MALDI-TOF**

The following results represent a descriptive study of the 2-D electrophoresis gel spots matched by MALDI-TOF analysis and database search. Results also are described in Figures 4-1 to 4-8 and sequence-matching results are summarized in Table 2.

At 7 DAA, the gel resolving the ER proteins revealed 16 spots, 7 of which yielded good MS spectra and were compared with database matches. Nine out of 16 spots visualized in the 2-D gel yielded no spectra. The gels were overstained to visualize as much protein as possible. However, the protein concentration in the faint spots was not enough to produce sufficient peptide concentration after trypsin hydrolysis. Spot 3 is protein disulfide isomerase (PDI). PDI is a multifunctional glycoprotein involved in the

formation and isomerization of disulfide bonds (-S-S-) in nascent secretory proteins as well as in assisting in a variety of protein maturation processes within the ER. It catalyzes the rearrangement of bonds in proteins (15). Spot 9 contains the putative NOD26-like membrane integral protein. Its function is a transmembrane transporter (16). Spot 11 is a putative salt-tolerance protein 5 named SOS3 protein. It binds to and activates the self-inhibited SOS2 protein kinase, which mediates the expression and activities of various transporters important for ion homeostasis under salt stress (17).

Spot 13 is cyclin A2, essential for the control of the cell cycle at the G1/S and the G2/M (mitosis) transitions, which is highly active at this stage of wheat growth (18). Spot 9 didn't match any protein in the present database.

Nineteen spots were visualized at 14 DAA in the ER fraction, among them the sequences of 10 spots were identified by database match search (Fig. 4-2). Spot 2 is defensin, specifically induced during cold acclimation in wheat. It inhibits protein translation in cell-free systems (19). Spot 3 is identified as putative eukaryotic translation initiation factor 2A. It functions in the rapid shutoff of host cell protein synthesis that occurs upon infection with selected viruses (20). Spot 9 is the starch synthase, in which subcellular components are in the chloroplast. Its function is starch biosynthesis (21). Spot 10 is phosphate/phosphoenolpyruvate, a translocator-like protein with a role in carbohydrate synthesis (22). Spot 18 is putative calcium/calmodulin-dependent protein kinase (CaMK), an ATP/calcium binder involved in amino acid phosphorylation (23). Three other spots didn't match any protein in the present database, although they were identified by the MS-FIT search. One spot was not identified by the MS-FIT search although an acceptable spectrum was seen for this spot.

At 34 DAA, the ER fraction of 2-D gel revealed 19 spots, 6 of which were identifiable by MALDI-TOF analysis and database search (Fig. 4-3). Spot 7 is a eukaryotic initiation factor (iso) 4F subunit, which is a nuclear ATP-dependent RNA-unwinding protein (24). Spot 10 is peptidyl-prolyl isomerase (PPI), which is an ER resident induced by heat shock. It is a PPIase that accelerates the folding of proteins during protein synthesis. This PPIase binds calmodulin (25). Three protein spots yielded no close match at the present time in the database.

At 60 DAA, the ER fraction resolution revealed 39 protein spots, 14 of them were identifiable (Fig. 4-4). Spot 2 is cytochrome P450 isoform, an ER resident protein involved in sterol biosynthesis (26). Spot 13 is a putative chlorophyll a/b-binding protein (CAB). Its role is in photosensory transduction within the photosynthetic organs (27). Spot 19 is an integral membrane protein from the acquaporin family. It functions as a transporter protein across membranes (28). Spot 21 is a putative GTP-binding protein RAB7D. It functions as a small GTPase mediated signal transduction integral protein (29). Spot 27 is putative protein tyrosine-serine-threonine kinase. The family of tyrosine-serine-threonine kinase is a group of nuclear proteins involved in DNA repair. Spot 30 is a putative nucleotide-binding site plus leucine rich repeats (NBS-LRR), a disease-resistance protein that plays a role in the cellular apoptosis expected at this stage of growth (30). Spot 31 is a putative DNA-directed RNA polymerase II 13.6K chain. Its subcellular localization is nuclear and it catalyzes the transcription of DNA into RNA using the four ribonucleoside triphosphates as substrates (31). Spot 34 is a putative multidrug-resistance associated protein, which is an integral-membrane protein whose role is in transmembrane movement of substances. Its subcellular localization is reported

to be in both the ER and GC membranes (32). Five other spots didn't hit any identifiable match.

Regarding the GC fractions, 2-D resolution of the 7 DAA fraction revealed 9 spots, 3 of them were identifiable (Fig 4-5). Spot 5 is a putative serine/threonine protein kinase, required for many functions; importantly, amino acid phosphorylation and membrane integrity (33). The putative wound-inducive protein identified on spot 6 is of unknown function (34). One spot hit no match.

At 14 DAA, 16 out of 40 appearing GC spots on the 2-D gels were identifiable. Three spots hit no match (Fig. 4-6). Spot 2 is imidazole glycerol phosphate dehydratase involved in amino acid biosynthesis (35). Spot 8 is alternative oxidase protein, which is a mitochondrial membrane protein involved in cellular respiratory exchange (36). Spot 10 is sucrose synthase type 2, involved in sucrose biosynthesis (37). Spot 22 is laccase, a secreted protein involved in lignin degradation and detoxification of lignin-derived products (38). Spot 23 is a putative nucleosome/chromatin assembly factor A, a nuclear protein involved in nucleosome assembly (39). Spot 24 is the starch-associated protein R1 known as starch dikinase, a chloroplast protein that functions as a general regulator of starch degradation (40). Spot 30 is Cw-21 peptide, non-specific lipid transfer protein, a membrane protein involved in the transfer of phospholipids as well as of galactolipids across membranes (41). Spot 32 is a previously described protein disulfide isomerase 2 precursor (15). Spot 35 is a multidrug-resistance associated protein MRP2, which is an integral membrane protein involved in transmembrane movement of substances (42). Spot 37 is the putative 2-oxoglutarate-dependent dioxygenase involved in DIMBOA-biosynthesis. DIBOA [2-hydroxy-2*H*-1,4-benzoxazin-3(4*H*)-one] and its methoxy

derivative DIMBOA are natural pesticides, serving as important factors of host-plant resistance against microbial diseases and insects (43). Spot 38 is a chlorophyll a/b-binding protein WCAB precursor, which is a membrane protein involved in photosynthesis light harvesting (44).

At the GC fraction of 34 DAA, 19 out of 63 appearing spots were identifiable (Fig. 4-7). Spot 19 is amine oxidase-related protein, a glycoprotein involved in the oxidative deamination of primary amines in plants (45). Spot 20 is a putative WRKY-type DNA-binding protein involved in the induction of many disease-resistance genes (46). Spot 23 is a membrane protein rich in hydrophobic residues, involved in potassium transport, which is the putative AKT1-like potassium channel (47). Spot 24 is the nucellin-like aspartic protease involved in proteolysis (48). Two spots, 25 and 26, are putative ubiquitin-conjugating enzymes involved in the ubiquitin cycle (49) and a proteasome inhibitor-like protein (50). Both are cytosolic proteins involved in protein degradation, which predicts that the process of malformed protein degradation is active at this stage of maturity. Spot 55 is the putative protein kinase, which is an amino acid phosphorylation enzyme (51). Spot 56 is a putative seed inhibition protein also known as putative raffinose synthase (52).

At the 60 DAA, from the 29 spots analyzed, 10 proteins were identified. Spot 1 is fatty acyl CoA reductase involved in lipid metabolism (53). Spot 2 is the photosystem I (PS I) reaction center subunit IV, a membrane protein that stabilizes the interaction between psaC and the PS I core, assists the docking of the ferredoxin to PS I and interacts with ferredoxin-NADP oxidoreductase. This protein is located in the chloroplast thylakoid membrane (54). Spot 4 is protein disulfide isomerase previously described in

the ER 7 DAA fraction as a multifunctional glycoprotein involved in the formation and isomerization of disulfide bonds (15). Spot 18 is ATP synthase beta subunit involved in hydrogen-exporting ATPase activity and phosphorylative mechanism (55). Spot 19 is a salt-inducible protein kinase functioning as protein serine/threonine kinase enzyme (56). Spot 20 is chloroplast nucleoid DNA-binding protein-like involved in proteolysis (57). Spot 28 is a putative transcription initiation factor, a nuclear protein component of the transcription factor IID (TFIID) complex, essential for mediating regulation of RNA polymerase transcription (58). Spot 29 is an AP2 domain transcription factor, like a nuclear protein involved in transcription (59).

DISCUSSION

The methodology of this study is aimed at identifying the constitutive proteins of the ER and GC, the major organelles of the secretory pathway at different stages of wheat growth. To perform this task, wheat endosperms were fractionated using discontinuous sucrose gradients and the resulting collected fractions were subjected to two-phase partitioning to remove contaminating plastids. This is the step to prepare enriched GC fractions, while for the ER , further steps were undertaken.

The total volume of the smooth ER is less than that of the rough ER throughout the stages of seed development of wheat. In addition, after vacuoles are filled with storage proteins, further deposition occurs within the lumen of the rough ER in a process of retention (60). Thus, the rough ER was selected in this study. The ER fractions were subjected to a second sucrose gradient centrifugation to separate the smooth from the rough ER fractions. The rough ER fraction was treated with puromycin to strip the membrane-bound ribosomes. The pattern of protein was analyzed by 1-D SDS-PAGE through different stages of fractionation. The fraction separation was analyzed by Western blot using enzyme markers specific for each organelle. The proteins from each fraction at all studied stages of growth were resolved by 2-D electrophoresis. Resulting protein spots were fingerprinted by MALDI-TOF and identified through database search. To the best of our knowledge, this is the first attempt to fractionate the organelle proteins of wheat endosperm using a sucrose gradient.

The pattern of weight change on a dry basis (Fig. 1) is in agreement with the pattern of protein concentration of the total crude extract (Cr Ex) of the three growth stages (7, 14 and 34 DAA) shown in Table 1, although the dry weight of wheat seeds represents all solids, including protein accumulation and other reserve materials such as starch. For 60 DAA, the BCA assay showed an increase in the protein content while the weight chart showed a slight decrease in fresh weight. The change in fresh weight is apparently due to a decrease in moisture content, observed at this stage of wheat growth. Data from both sources (BCA and SDS-PAGE) revealed a significant increase in protein content between 7 and 14 DAA. A higher protein content was observed, between 14 and 34 DAA compared to other development stages. After 34 DAA the grain filling appears to plateau in the weight determination chart. Those results were predicted by other studies (5, 14) and are also in agreement with the data obtained from the SDS-PAGE figure (Fig. 2).

Evaluation of Protein Recovery Rates during Fractionation

The enriched the ER fraction shows the higher protein recovery at 14 and 34 DAA, 4.7 and 4.2% respectively while the enriched GC fraction appears to have similar protein recovery (1.7 and 1.6%). This suggests that at this stage, the ER appears more active in synthesizing proteins and the GC keeps up about the same protein trafficking.

The highest total protein content was found at 34 DAA in the enriched ER and GC (4.2 and 1.6 mg/ml respectively, Table 1). Thus, a relatively lower protein recovery but higher protein content in the ER at 34 DAA suggests lower efficiency of protein fractionation. This may be due to deficiency in the following steps: 1) higher

contaminants in the crude extract compared to other stages of development, i.e. more protein per sample weight; and 2) removal of ribosomes from the rough ER further compromised the recovery process. With higher protein synthesis, higher ribosomes numbers are bound to the ER membranes and may contribute to lower efficiency upon fractionation and 3) higher fragmentation of the ER in the homogenization of these samples.

Effect of Contaminants on the Recovery Rate

The effectiveness of the fractionation of the ER and GC from wheat endosperm was influenced by cellular components that affect the density of the initial crude extract. Among these components are the soluble-starch protein particles (small starch granules and damaged starch) and a number of cytosolic proteins. The density of a medium depends on the solvent and amount of solids suspended or dissolved (61). Variations of the latter might have affected the fractionation efficiency.

The total amount of recovered protein at the final enriched stages ranges between 0.5 to 4.5% of the initial crude extract protein concentration. The high yield in organelle extraction is inversely proportional to the rate of organelle enrichment. A basic condition of a high ER and GC organelle recovery is an effective homogenization of the initial extracting material. Homogenization generally results in breakage of the plasma membrane, vacuoles, and mitochondrial membranes, eventually releasing the outer mitochondrial membranes, and lisosomes to the extraction medium. All of these structures contribute to impurities when fractionating ER and GC organelles. The risk of ER and GC contamination is high due to a density overlapping between these organelles and other vesicles (61).

During the homogenization procedure, a significant quantity of cytoplasmic proteins attach to the membrane surfaces contributing to about 30% of the total microsomal protein. Protein enrichment is usually achieved by differential solubilization or sedimentation (61, 62). In this study the amount of crude protein removed by two-phase partitioning was more than 80% of the original crude extract protein in all fractions of the four stages of growth. The protein determination assay (Table 1) shows that the removal of contaminants from the 7 DAA fraction by the two-phase partitioning and other measures (explained by the fractionation procedures from crude to enriched organelles) was about 99% of the ER and about 92% of GC. The organelle protein pool at this stage is still small compared to later stages of development. The 14 DAA lost about 85% of the ER-protein fraction and 88.5% of GC fraction. Concerning the 34 DAA, the two-phase partitioning removed about 86% from the ER fraction and about 91.6% from the GC fraction. The 34 DAA enriched fractions shows a lower recovery rate but higher protein content than the 14 DAA. Finally, the 60 DAA lost about 94.8% from the ER fraction and about 96% from the GC. Provided that the fractionation procedure is efficient, the lower recovery rate of protein can suggest that more contaminants in the enriched fractions have been removed. The lower recovery rate and the higher content of organelle protein at 34 DAA suggest that a larger pool of organelle protein exists in spite of higher removal of contaminants.

Effect of Homogenization-Induced Fragmentation on the Recovery Rate

Figure 5 shows the results of the fractionation methods used to separate both organelles, ER and GC, from wheat at different stages of growth. The cellular organelles vary greatly in size and shape. The ER and the GC belong to a class of organelle

structures consisting of flattened cisternae, which are prone to fragmentation during harsh homogenization procedures into small vesicular structures lacking a standard shape or size. This occurs in such a way that the cisternal content mixes with the cytosol, adding a further complication in the process of their separation from the rest of the cytosolic organelles (7). This may in part explain the lack of similarity in the SDS-PAGE between the ER and GC at the enriched level of 34 DAA, where the organelles have the largest pool of proteins and are more prone to fragmentation during homogenization. The 60 DAA enriched fraction, though fragmented, is still showing some resemblance to the crude extract. This result can suggest that both homogenization and desiccation may be different in their effects on organelle fragmentations.

Unlike many other cellular organelles, less than half of the lamellar and cisternal structures of the rough and smooth ER can be separated in an intact form that may relatively compromise, but not completely prevent, the reproducibility of band appearance during SDS-PAGE separation (7). In this study the SDS-PAGE band reproducibility was about 70%.

Besides, the homogenate usually contains unbroken or partially broken cells and may also contain aggregate material that takes place during nuclear lysis (61). Those aggregate materials may end up binding to the organelles and consequently co-banding with them during separation.

Effect of Organelle Properties on Protein Recovery Rate

One factor that affects the recovery rate of protein during fractionation is organelle density. Since both the ER and GC organelles are surrounded by semipermeable membranes, their density is not uniform and depends on the molecular

interaction between the organelles and the extraction medium surrounding them. The surrounding semipermeable membrane structures enclosing the ER and GC are dynamic in that they allow water and a small number of other molecules to pass freely across, while the flow of other materials is partially (unidirectional) or fully restricted. Constitutive proteins of membrane are one example of materials within the interior of the organelles that cannot diffuse outward (61).

Due to the dynamic property of semipermeability, the protein contents of intact membranes do not mix with other cytosolic proteins and this is the key element in confirming the authenticity of the isolated intact organelle membranes (61). Consequently, the cumulative mass of these organelles will be the mass of the membrane itself plus other membrane-bound structures: ribosomes, the non-diffusable solute trapped inside the organelle, and the mass of water and other diffusible solutes. This process will definitely affect the organelles' density and the fractionation process (63).

During high-speed centrifugation, the density of the particle equilibrates with the density of the sucrose gradient, and the particles will band at the buoyant density point. An organelle particle that is suspended in a liquid having its own density has no weight and will neither float nor sink (61). Because the GC is higher in density than the ER, both organelles will band during sucrose fractionation at different buoyant-density points. The ER will band at a higher interphase in the centrifuge tubes than the GC.

The sucrose steps gradient of this study was formulated for banding organelles at different interphases, taking advantage of the unique property of differential density of organelles. The two interphases represent a borderline between a sucrose solution that is less dense than the organelles and another one that is denser. This may explain in part the

initial observation in Figure 5, in which the two organelle fractions banded at two different levels, with the GC fraction being the denser fraction. This fractionation successfully separated the mitochondrial extract at the bottom of the tube from the GC fraction, which banded at a lower level than the ER fraction. In addition, the top layer of the fractions contained a fat layer and other low-density particles.

The addition of KCl/CsCl to the extraction buffer will exert a moderate osmotic effect, partially drawing water out of the cell medium, which consequently leads to a relative increase in concentration of the natural solutes within the organelles (61). This would in turn increase the density of the material within both the ER and GC, simultaneously decreasing its size. In conclusion, the addition of KCl/CsCl is a contributing factor in adjusting the density of organelles during fractionation to approach the theoretical values and consequently facilitate their extraction by sucrose gradient procedures.

Effect of the ER -Bound Ribosomes on the Recovery Rate

Rough ER contains cellular components affecting its density. The RNA of the membrane-bound ribosomes can constitute up to 60% of the total cellular RNA. More than 50% of the total RNA is sedimented with the nuclear and mitochondrial pellet, along with the ER (61), which reflects a significant loss in the ER and further compromises the recovery rate of proteins at the enriched level of the ER.

Optimization of the Two Phase Partitioning

The two-phase partitioning system separates membranes based on their surface charge, while sucrose-gradient separation is based on intrinsic density. In this study the two-

phase polymers were prepared as a stock of 20% DEX and 40% PEG. One important problem in preparing a good stock solution of these polymers was determining the moisture content of each polymer. A moisture content of 7.5% in DEX and 10% in PEG kept at 4 ºC has been reported (64), but moisture content could vary according to manufacturing and storage conditions. In this study the polymer concentration of the stock solution was adjusted using a refractometer.

To obtain membranes with a minimum of plastid contamination, it is necessary to optimize the phase composition of the two-phase partitioning. Morre at al (6) reported that at the polymer concentration of 5.9% (w/w) for both polymers (DEX and PEG), the plastids partitioned into the upper phase while the membranes of the ER and the GC partitioned into the lower phase. At a higher polymer concentration than 5.9% the risk of plastid contamination increases significantly, while at lower concentration the risk of reducing the yield of the desired membranes is likely due to their partitioning into the upper phase (7). In the current study, the partitioning of Cr ER and Cr GC from wheat endosperm showed a different phenomenon from the one described by Morre at al (6) for spinach-leaf fractionation.

The application of the two-phase polymers at a concentration of 5.9% yielded a green-yellowish precipitate similar in color to the upper-phase partition. The nature of the precipitate at this concentration was not investigated. The problem was solved by testing a series of DEX and PEG concentration. Sixteen concentrations were tested, ranging from 5.0 to 6.5% polymer with increments of 0.1% per tube. At a concentration of 5.0% almost no partitioning was found. Partitioning started at a concentration of 5.2% but showed very little particle dispersion. Partitioning increased at higher concentrations of

polymers. At concentrations above 5.6% the green-yellowish precipitate was formed. It was concluded that the best concentration of polymers leading to the least precipitation possible is at 5.6% DEX and PEG.

The surface tension of the interphase during the two-phase partitioning is very small and, consequently, no destruction of organelles occurs by surface denaturation at the interphase. The distribution between the two phases of a partitioning system is influenced by many factors, including:

1. Polymer concentration: The higher the polymer concentration (i.e. DEX and PEG), the higher the particle deposition is in the lower phase.
2. Buffer composition: When buffer is present in the two phases, an electric potential is formed between the two phases. Different ions in the polymer mixture will have different affinity for the two phases and particles will be preferentially distributed in the system according to their charge properties. The electric potential can be adjusted by changing the buffer composition and concentration to control the partition (63).

Evaluation of the Sucrose Fractionation Method

There is no previous report about the use of this fractionation procedure for wheat-endosperm organelles, which makes this study the first to report such results. The basis of the enrichment of the ER and GC was a sucrose fractionation, two-phase partitioning (DEX and PEG) and 2-D electrophoresis separation of the complex mixture of proteins based on isoelectric point (charge) and molecular size. The purpose of selecting the sucrose-gradient methodology for the organelle separation was its relative ease of preparation, application and removal. Sucrose

is a true solute, so membranes can be harvested from sucrose solutions by simple dilution of the medium with two or three volumes of buffer (7, 61).

Several conclusions could be drawn from the SDS-PAGE pattern of the fractionation steps. As expected, maturation stages of wheat endosperm bring more protein synthesis and vacuolar filling. Consequently, more contaminant proteins are expected to be found during the fractionation of the ER and GC proportional to the stage of growth and maturation. The SDS-PAGE shows that 7 DAA has the less protein and the 34 DAA has the most because at this stage protein synthesis and grain filling is at maximum. The original crude extract at 7 DAA shows a basic similarity to that of the 14 DAA, possibly because both represent the developmental stages of early grain filling. It is expected that more protein synthesis takes place at 14 DAA. However, the SDS-PAGE analysis only revealed the appearance of 2 new bands at 75 and 100 kDa. The crude extract at 60 DAA is an exception to the expected trend of more protein bands due to the process of grain desiccation, which fragments the organelle proteins, leading to the loss of the turgent state during development.

Mature endosperm has organelles more likely collapsed during the desiccation period at maturity and this may explain the organelles' lower protein content at this stage. Farrant et al. (65) reported that in desiccation-sensitive plant cells, plasma membranes were discontinuous and the organelles had lost integrity. Another study reported that organelles with a single membrane (ER and GC) were first destroyed during programmed cell death of wheat seedlings, and then the organelles with two membranes (mitochondria and chloroplasts) were degraded. During the process of organelle destruction, the matrix was first destroyed, the organelles swelled, and then the integrity of the membranes was

damaged. It is assumed that auotophagy takes place during degradation of cellular organelles (66).

Similar to Cr EX, the Cr ER and Cr GC show their protein patterns proportional to the stage of development (Fig. 2). Less protein banding during the sucrose gradient fractionation is shown at the 7 DAA than at 14 or 34 DAA. Since maturation of endosperm is bringing more vacuolar and organelle filling, the sucrose fractionation is showing more protein banding in crude organelle fraction proportional to the maturation stage. The crude organelle fractions at 34 DAA (both and Cr GC) appear to have some protein pattern difference compared to other fractions. This is the stage where the organelles have an apparent differentiation compared to other stages of growth. These crude fractions appear the highest in concentration and the more diverse in protein pattern among all fractions.

During endosperm maturation, protein deposition intensifies in storage vacuoles, which lead to vacuolar full development. Around 34 DAA, saturated vacuoles lead to the deposition of small vacuoles within the lumen of the ER, which may further fuse, finally forming a central vacuole, in which protein bodies are sequestered. These protein bodies apparently continue to enlarge by fusions, with each forming large bodies surrounded by the ER (67). The mechanism by which the ER-surrounded protein bodies enter storage vacuoles is not well understood, since protein bodies are much larger than the GC, which makes the GC less likely to be involved in their transport (68). Consequently, it is possible that either the same proteins are present in a larger amount or different proteins are present at this stage, or both; and more contaminant proteins will co-band with the

organelles during fractionation, explaining in part the diversity of the crude organelle fractions at 34 DAA.

A possible explanation of the lower protein concentration and pattern at 7 DAA crude organelles is that the organelle system is still in its initial stages of development and relatively less protein is being synthesized by its machinery, so less protein co-bands with the organelle fractions.

The same sucrose gradient step used in spinach-leaf fractionation (6) was reported to precipitate the mitochondrial proteins in the pellet. Some of the low molecular weight proteins (below 30 kDa) removed from the crude extract by sucrose fractionation could have included mitochondrial proteins. The mitochondrial proteins include an 8 kDa ATP synthase protein (69), a 28-kDa mitochondrial S7 ribosomal-homologue protein (70)**,** a 12 kDa mitochondrial S12 protein (71), a 14.5 kDa mitochondrial ribosomal protein S13 (72), a 32 kDa ADP/ATP carrier protein (73), a 34-36 kDa isomers outer mitochondrial membrane protein, porin (74). The protein elimination between the 37 and 60 kDa could also suggest the removal of some mitochondrial proteins such as the 42.5 kDa subunit of the NADH: ubiquinone oxidoreductase (complex I) (75). The remaining low molecular weight in the crude fractions could possibly be vacuolar or ribosomal proteins.

The role of the two-phase partitioning is to eliminate contaminant proteins that co-banded with the organelle fraction in the sucrose-gradient phase. The two-phase partitioning was as effective in removing substantial amounts of proteins in all immature stages. An additional step was undertaken in the ER fractions, which is the removal of the ribosomal proteins associated with the rough ER fractions. The elimination of contaminants is showing a differentiation in the protein pattern of enriched organelles in

the 34 DAA, possibly due to increasing function proportional to the maturation stage. The enriched 34 DAA fractions appear to be the densest fractions among all in terms of band distribution. Interestingly, the 60 DAA fractions appear to be different in both the ER and GC fractions from immature fractions, especially at the low-molecular-weight portion, due to the fragmentation of many peptides resulting from the effect of endosperm desiccation at this stage of growth. The effect of desiccation may be visually predicted from the accumulation of the low-molecular-weight peptides shown at the bottom of the SDS-PAGE gel (Fig. 2).

The elimination of the remaining low-molecular-weight proteins from the crude fractions of both organelles is possibly due to the removal of vacuolar and ribosomal proteins. A SWISS/PROT database search demonstrates that many vacuolar proteins are in the low-molecular-weight range. Based on their molecular weight, some probable candidates are a 21 kDa putative plastid ribosomal protein CL9 (76), a 21 kDa plastid NAD(P)H-quinone oxidoreductase chain I (77), a 23 kDa plastid 2-cys peroxiredoxin BAS1 (78), a 26 kDa small heat shock protein (79), a 27 kDa plastid envelope membrane protein (80), a plastid 28 kDa chlorophyll a-b binding protein (81), a and 34 kDa chloroplast oxygen-evolving enhancer protein 1 (82).

Similarly, most ribosomal proteins like the group of 50S (L2, L14, L16, 20, L22, L23,L 32, L33, , L36), the group of 60S (L35), and 30S (S2, S3, S7, S8, S11, S12, S14, S15, S16, S18, S19) have molecular weights ranging between 8 and 34 kDa (83). Since the two-phase partitioning of the ER fractions showed the removal of low-molecular proteins of this range, these ribosomal proteins could be candidates for elimination.

Lippintcott-Schwarz at al (84) reported that the whole secretory pathway is structurally similar in term of membrane composition. The similarity is suggested to be the effect of vesicular proteins shuttling between the two compartments. Nascent proteins synthesized in the ER are transported to the GC by special coat proteins that bud from the ER exit sites and fuse with the pre-Golgi compartment. In reverse, enzymes and other ER-resident proteins that escape from the ER lumen are detected by specialized domain within the GC and are shipped back to the ER. Our results suggest that both enriched fractions ER and GC have a degree of protein pattern similarity within the particular stage, especially between 30 to 60 kDa. Some protein bands (about 30 and 35 kDa) are even identical among enriched fractions across all stages of development. A potential candidate is an ER-Golgi intermediate compartment with a MW of 32 kDa protein. Other common proteins for both compartments are a group of ER-to-Golgi transport-related proteins with a range of molecular weight, 34-37 kDa (85).

At the 7 DAA the differences were observed in the high-molecular-weight protein fraction (between 65 and 70 kDa forthe ER and one band at 70 kDa for GC). The probable ER proteins of this MW range could be protein disulfide-isomerase EUG1 precursor, which is about 65 kDa, and endoplasmic reticulum lumenal Ca (2+)-binding protein grp78, which is about 72 kDa (86). One GC protein candidate could be a 70 kDa Golgi-localized, gamma ear-containing, ARF-binding protein 1 (87).

At 14 DAA, the difference in protein expression between enriched ER and GC is in three bands at 50, 65, and 70 kDa in the ER and two bands of 100 and 90 kDa in the GC. At this stage the differentiation in function may not have started yet, as shown in the 34 DAA. The bands at 65 and 70 kDa may be identical to the ones appearing in the 7

DAA. The closest known ER protein to the 50 kDa band is a 47 kDa Omega-3 fatty acid desaturase (88). Probable proteins for GC are Golgi adaptor HA1/AP1 adaptin gamma subunit clathrin assembly protein complex 1 gamma large chain gamma-ADA of 92 kDa (89) and Calcium-transporting ATPase (90) of about 100 kDa.

At the 34 DAA stage, the protein profile becomes different, probably due to the shift in the utilization of different components of the secretory pathway. In addition, at the time of full development of the functional proteins (34 DAA), the effect of organelle fragmentation due to homogenization and protease activity may be responsible for displaying dissimilarity in both organelles at the enriched level. The effect of homogenization-induced fragmentation on the protein appearance in the SDS-PAGE is different from the effect of protease fragmentation in that the homogenization was reported to break the organelles' integrity, but may not induce organelles lysis (61); while the lytic activity of protease includes a fragmentation of protein into constitutive peptides. The difference in protein pattern between the ER and GC refers to an additional expression of proteins between 90 and 120 kDa of the ER fractions. Among possible protein candidates are a 120 kDa eukaryotic translation initiation factor 2-alpha kinase precursor (91), a 111 kDa calcium-transporting ATPasethe ER type (92), a 90 kDa putative cell-division-control protein 48 homolog D (93). Other bands seem common to the 14 DAA ER proteins. The GC fraction has a 20 kDa-expressed band not appearing in the ER. This band is not also appearing in the GC of 14 DAA. Many GC 20 kDa candidates are possible, including an 18kDa clathrin coat assembly protein AP19 (94).

Though some protein-pattern similarity appears at 60 DAA, a conclusive protein pattern of organelle similarity cannot be predicted from the 60 DAA due to fragmentation of the organelles.

Though differences in protein patterns in the fractionation step of the crude extract to yield crude organelles were observed in the form of band elimination and enrichment, differences in protein concentration were not observed in the SDS-PAGE. The fractionation step fror the crude extract to the enriched organelles showed a process of band elimination as well as reduction of protein concentration. In the protein content assay (Table 1) all fractionation steps showed a reduction in protein concentration proportional to the stage of fractionation. Consequently, direct comparison of protein concentrations (BCA method) and protein-profile patterns (SDS-PAGE) couldn't be done from this study. Among the challenges to overcome in future research is the limited solubility of the proteins and the hydrolysis to smaller peptides. Both factors could have affected the results. For example, small molecular weight peptides would have been determined as proteins in the BCA method, while insoluble proteins and small-molecular-weight peptides (< 10 kDa) may not be completely resolved in the SDS-PAGE gel.

Morre at al reported a successful sucrose fractionation for the separation of the ER and GC in green leaves (6, 7). However, no previous studies reported fractionation results of wheat endosperm. The fractionation of the ER and GC from green leaves was assessed by electron microscopy imaging using a similar fractionation and showed that the preparations were relatively enriched. The authors reported that the ER fraction consisted of 80% ER plus a minor fraction of other particles, while the GC fraction consisted of 65% stacks of cisterae with some contaminants due to co-banding of the ER

particles. Other contaminants include plasma membrane vesicles (15-20%), thylakoids (10-15%) and some unidentified vesicles (10-15%) (7).

In this study, the success of ER and CG enrichment was tested by Western blot analysis (Fig. 3), which has not been reported before. The ER fraction, CRT enzyme marker, showed an average of three times the band size compared to the GC fraction, confirming some co-banding of ER particle with the GC. When testing for the GC enzyme marker (FTCD), no ER protein fragments were found. Thus, the enriched ER fraction appears to be free of GC but cellular components could still potentially be present.

Results of Proteins Resolving by 2-D Electrophoresis and MALDI-TOF

The descriptive study of the constitutive proteins of the ER and GC organelles at different development stages of wheat endosperm is a preliminary attempt to build a comparative database for protein expression found during grain filling. A comparative study of the differential expression of proteins between these developmental stages was not the aim of this work and will be the focus of future research. To the best of our knowledge no descriptive or comparative database exists for the ER and GC of wheat. The only study we came across was one comparison of the whole-wheat endosperm protein expression at 17 and 45 DAA (12).

As expected, 2-D (Fig. 4) separation revealed an increasing number of resolved bands as the DAA (developmental time) increased. A similar trend was observed in 1-D SDS-PAGE and BCA assay of protein content. For each stage of growth all the detectable protein spots revealed with silver staining were analyzed. A total of 85 spots (36%) were identifiable out of 234 spots detected in 8 silver-stained gels (Table 3). Spots

identified from the ER fractions across development stages were 37 (40%) out of 93 gel spots. Spots identified from the GC fraction were 48 (34%) out of 141.

The constitutive proteins of the secretory pathway are not exclusively made of membrane proteins, but the membrane is the major fraction in these organelles. The pattern of protein resolution in all samples still poses the challenge of membrane protein solubility and stability of this solubility during the extraction and analysis. Similar challenges in membrane solubility were previously reported (95). Apart from disulfide bridges, other major types of forces holding proteins together are non-covalent interactions: ionic bonds, hydrogen bonds and hydrophobic interactions (96). Consequently, a successful solubilization medium should be able to break all these bonds and interactions.

The remarkable observation in the 2-D gels was the presence of large protein spots, presumably due to limited protein solubility. Except for 2 fractions (GC fractions at 14 and 34 DAA), all gels showed intensive band-distribution patterns around the edges of the pH range. Those observations revealed some challenges in the Isoelecrtical Focusing separation. The presumed low solubility of membrane proteins led to two major kinds of spots appearing on the gels: large unresolved lumps and small-sized, faint spots. The small-sized spots were mostly below the detection level of MALDI-TOF. These results were due to the low concentration of protein in the faint bands. The in-gel digestion procedure used was highly effective in demonstrative assays.

The two exceptions for this pattern are gels for 14 and 34 DAA GC fractions (Fig. 4-7 and 4-8), which showed a lower number of large lumps and small spots relative to other gels. However, the rate of identifiable spots in the 14 DAA fraction was 40%,

which is moderately higher than the cumulative rate of identified spots (36%). The rate of the identifiable spots in the 34 DAA fraction was not higher than the average rate of spots. The majority of spot distribution in those two fractions remains at the edges of the pH range. These observations suggest that the relatively better-resolved spots in these two fractions didn't improve the level of identification, presumably due to a still-existing low solubility of membrane proteins.

The pattern of spot distribution in the ER fractions showed a relative resemblance between the 14 and the 34 DAA fractions, while the fractions of the GC didn't show any resemblance in protein distribution among the development stages. The 2-D electrophoresis of the 7 DAA ER proteins showed a trend of similar molecular-weight protein distribution to the 1-D electrophoresis in the upper range of molecular weight (100-65 kDa). The low-molecular weight spots (below 30 kDa), although appearing in the 1-D electrophoresis, are not well observed in 2-D of the ER at 7 DAA (one spot), while they are more apparent in the GC. This is possibly due to a lower solubility of the ER proteins compared to the GC proteins. The 7 DAA GC protein distribution in 2-D shows a limited trend of resemblance to 1-D protein distribution, especially at the lower molecular-weight range of 40-20 kDa. The 1-D spot of the same fraction are clustered in the middle range of molecular weight (75-50 kDa). Although the lower molecular-weight spots shown in the 2-D of GC due to the more sensitive silver nitrate staining are not showing in the 1-D, they may still be present but not visualized.

At 14 DAA both the ER and GC fractions show a trend of protein distribution similar to the distribution trend observed in 1-D electrophoresis for the same fraction. However, more proteins are seen in the GC fraction compared to the ER, although this

protein distribution is similar in the 1-D. Similar observations were drawn from the 34 DAA ER and GC fractions where more protein distribution is seen in GC fraction compared to the ER, while the 1-D is showing the opposite pattern. This may be due to the more hydrophobic nature of the ER compared to GC, a phenomena that is common to all immature stages of wheat-endosperm development.

Concerning the 60 DAA fractions, both fractions show a comparable trend of protein distribution between the 1-D and the 2-D electrophoresis. In addition, both fractions appear to be similar in the 2-D electrophoresis separation. This is the stage of endosperm desiccation where organelles lose their integrity and structure. Possibly the protein pattern seen at this stage no longer reflects the organelles' original resident proteins.

The cumulative results of the 2-D analysis suggest more protein distribution in the GC fractions of immature stages compared to the ER, possibly due to a higher hydrophobicity of the ER leading to a lower solubility in the 2-D gels. The higher content of ER proteins compared in the 1-D electrophoresis is probably due to different solubilizing procedures used in the two kinds of electrophoresis.

Speculated Factors Compromising the 2D Results

The major challenges that compromise a successful 2-D resolution of membrane proteins take place at two stages. The first takes place during the initial solubilization process of the samples, where important interactions occur among a variety of membranous proteins with different pH, or between those proteins and other interfering agents, such as salt residues from the extraction buffer. The second stage is during the

entry of the sample into the gel matrix of the focusing strip and the stabilization of protein inside the strip after their entry. At this stage there is a stacking effect due to the protein transition from the liquid phase to the gel phase. This stacking increases the friction coefficient, possibly resulting in an increased precipitation of proteins instead of their entry into the gel matrix, due to the clogging of the gel pores and poor penetration of the bulk of the proteins (96).

Membranous protein is the major fraction of proteins in the fractionated organelles (ER and GC). It is speculated that the ER is more hydrophobic than the GC. For membranes, the gross structure of proteins is driven by hydrophobic interactions. The strength of these hydrophobic interactions may be the clue to the challenges encountered in 2-D electrophoresis with the Immobilized pH Gradient (IPG) that was used in our procedure. In this procedure, the proteins were solubilized in a buffer containing a strong chaotropic agent, a suitable detergent and an ampholyte buffer. The role of chaotropes (usually urea and thiourea) is intended to disrupt the hydrogen bonds, but this would lead to the exposure of the hydrophobic portions of proteins by unfolding their hydrophobic core, resulting in an increased potential for hydrophobic interactions. This may have a compromising effect on the solubility of our fractions, especially on the ER due to its strong hydrophobic nature. The role of detergents, in return, is to provide a stable dispersion of the exposed hydrophobic cores of membranes. This takes place by coating the proteins to make them more hydrophilic in order to prevent their precipitation. Also, the role of the detergent may be compromised in the case of membrane proteins because the hydrophobic area is too large, which decreases the critical micelle concentration and thus the concentration of the detergent available (96).

Even in the case of successful protein solubility, membrane proteins may re-precipitate once they reach their isoelectric point due to their loss of net charge, which cancels the electrostatic repulsions and promotes aggregation and precipitation (96). Sample residues were found in the strip holder at the end of the focusing procedure, with the holder for the ER samples containing more residues. This observation raises two possibilities, low solubility or a reprecipitation event. Even if proteins do not precipitate following the loss of their net charge, they lose their ability to migrate within the second dimensional gel (96). The latter possibility was ruled out because a silver staining of the gel strips didn't reveal any protein residue in the strips, which suggest that either the proteins didn't enter the gel strip or they reprecipitated after entering.

Another speculated challenge that may have compromised our 2-D results is the salt residues (96) that may be coming from buffers used at different steps of the fractionation. Our extraction buffer contained many salts, including potassium, sodium and chloride. Salts originally do not interfere through their binding to proteins; rather they interfere through the electrophoresis process. Salts are reported to migrate through the pH gradients and accumulate at both ends of the electrophoresis poles. This accumulation builds very high conductivity zones, the size of which will depend on the salt concentration. Due to the high conductivity, the voltage drops and so does the electrical field of these zones. Consequently, proteins cannot focus in these zones (96). Nearly all of our 2-D gels of the ER fractions showed lump accumulations near the edges of the pH range. This phenomenon was less in the GC fraction.

In conclusion, the challenge we faced during the 2-D separation may have risen from a combination of factors, including the organelle protein hydrophobicity and salt traces from extraction buffers.

Description of Important Organelles Makers at Different Stages of Endosperm Development

The results of the 2-D electrophoresis revealed the presence of proteins that are markers of the separated organelles. The PDI enzyme is particularly important. Other proteins found are either nuclear or cytosolic resident proteins. Since the ER and GC are the major organelles for protein synthesis, these proteins may be residing within the specific organelles at the time of fractionation. Some of the identified proteins represent the hallmark of developmental stages in wheat. The following discussion will focus on the anticipated role of these proteins during a particular stage.

PDI is a member of the thioredoxin superfamily, and is highly abundant in the ER-luminal protein fraction, constituting approx. 0.8% of total cellular protein. The protein, about 510 amino acids in length, carries a typical C-terminal KDEL ER-retrieval sequence for the retrograde activity of protein export for the ER. PDI is a catalyst of the rate-limiting reactions of disulphide-bond formation. It also catalyzes isomerization and reduction within the ER, and it displays chaperone activity. Catalysis of disulphide-bond formation can occur cotranslationally (15, 97). A chaperone is a protein that can assist unfolded or incorrectly folded proteins to attain the native state by providing a micro-

environment in which losses due to competing aggregation reactions are reduced, and which mediates the reversibility of pathways leading to incorrectly folded structures. In its role as a chaperone, PDI interacts with malfolded proteins or endogenous, nascent proteins. Its function is to help folding and protect nascent protein during their translation events. In addition to their location in the ER lumen, proteins from the PDI family may also be found in different compartments as the chloroplast-specific PDI in plants that regulates the light-induced translation of chloroplast mRNAs through redox activity (97). In this study, the PDI was identified in more than one stage of development. Interestingly, it was also identified in the GC fraction at 14 DAA, which predicts a role of this enzyme in the post-translational activity of GC.

Other important enzymes in wheat endosperm development are the starch synthase enzymes, the function of which is to add glucosyl units at the nonreducing end of linear chains through new α(1→4) linkages (21). Though the isoform III was identified in this study, five subfamilies of starch synthases have been identified in higher plants, including granule-bound starch synthase (GBSS), starch synthase I (SSI), starch synthase II (SSII), starch synthase III (SSIII), and starch synthase IV (SSIV) (98). The role of startch synthase III appears to be primarily in amylopectin biosynthesis (21), which suggests its presence at 14 DAA. Though the starch synthase III is localized in the stroma of plastids, plant organelles vary greatly in the classes they possess and in the relative contribution of the classes to soluble starch-synthase activity (98). Though it is not clear whether individual isoforms of starch synthase make qualitatively different contributions to amylopectin synthesis, the mutation of SSIII resulted in the loss of almost 80% of the soluble activity of the potato tuber, causing deep fissuring of the starch granules. These

results raise the possibility that there are qualitative as well as quantitative differences between plant organelles in the contributions of individual isoforms of starch synthase to the synthesis of amylopectin (98).

Another remarkable identified protein in this study is nucellin-like aspartic protease. It is involved in the nucellar cell degeneration in flowering plants. It has the essential features of aspartic proteases of the pepsin family. It has two catalytic sites, one in each of the N- and C- terminal regions. Nucellin has two possible roles in the nucellar cell death. It functions as an apoptotic protease and as a major hydrolytic protease that converts the cell-death proteins into the nutrients for endosperm development. This enzyme was identified at the 34 DAA GC fraction. Along with identification of the putative ubquitin-conjugating enzyme, it is suggested that at this stage the programmed cell death and endosperm desiccation are about to become active (99).

CONCLUSION

The developed fractionation and enrichment methods yielded enriched extract of the ER and GC from wheat endosperm at four stages of growth, 7, 14, 34 and 60 DAA. Western-blot immunodetection using CRT and FTCD as markers for the ER and GC respectively confirmed that the sucrose gradient fractionation combined with the two-phase partitioning separated the two organelles (ER and GC). The weight-change pattern across stages of development showed an increase in seed weight across time, with the 7 DAA and the 34 DAA being the lowest and the highest in seed weight. These results are in agreement with previous studies. The protein content of crude extract of all fractions was in agreement with the weight-change pattern of seeds. The results suggest that these four stages represent different functionalities of the organelles.

The band distribution on the SDS-PAGE showed a pattern of enrichment proportional to the stages of fractionation, with the enriched fractions containing the lowest pattern. The exception to this result was the 60 DAA fraction due to the process of organelle fragmentation at maturation. A change in the protein pattern can be observed in the SDS-PAGE for the fractionation step yielding crude and enriched organelles. However, a change in protein concentration can only be observed in the fractionation step yielding enriched fractions.

In SDS-PAGE the crude extract of 7 and 14 DAA show some protein-pattern similarity, possibly due to the fact that both are early stages of maturity. The crude extract of the 34 DAA seems the most concentrated due to organelle and vacuolar maturation.

Some degree of similarity was observed in the same organelle across stages between 30 and 60 kDa, suggesting an existence of proteins with comparable molecular weight within the corresponding enriched fractions. SDS-PAGE also showed that some protein masses are common to all enriched fractions, presumably proteins of transport vesicles common to both the ER and GC.

While the 14 DAA showed some remarkable development in band density compared to 7 DAA, the highest enriched fraction in band distribution was the 34 DAA, which suggests the highest activity of protein trafficking at this stage of grain filling.

Previous studies reported that the ER and GC are structurally similar due to the presence of proteins shuttling between them. Enriched fractions of the ER and GC show a larger trend of similarity among each other at 7 and 14 compared to the 34 DAA. Different protein profiles among the ER and GC at 34 DAA suggests a homogenization-induced fragmentation as well as a possible sign of shift in the utilization of various organelle proteins during grain filling. The different protein pattern at 60 DAA may reflect a process of desiccation-induced fragmentation of the organelles.

The 2-D electrophoresis revealed a relative pattern of homology between ER fractions confirming the results of the SDS-PAGE, while this homology couldn't be confirmed in the GC fraction. A group of 234 protein spots were visualized on the 2-D gels from all stages of development, with 85 (36%) of them identifiable by MALDI-TOF

and database search. The identifiable spots contain a number of organelle-membrane proteins from the ER and GC, suggesting a success of the process of fractionation. The presence of other proteins is possibly due to their residence in these organelles at the time of fractionation. The identifiable spots represent the first step of a descriptive study of wheat organelle proteins at different stages of growth. The optimization of a descriptive study could be used as the foundation for a comparative database for differential expression of organelle proteins at different stages of growth, from which a number of complex systems could be described and their functions studied. Of specific interest are those proteins with landmark activity at specific stages of development, such as the disulfide isomerase (PDI), important in protein folding at early and middle stages; starch synthase, important at middle stages where storage material starts accumulating; and proteases, important at late stages of development where programmed cell death becomes active. Although the fractionation was successful, 2-D resolution of enriched ER and GC needs to be improved; specifically in improving the solubility of membrane proteins of the obtained fraction of the organelles.

RECOMMENDATIONS FOR FUTURE WORK

A. Improving the sucrose gradient fractionation techniques:

Several hypotheses could be tested to improve the yield in the sucrose-gradient fraction. The first hypothesis is that changing the sucrose-gradient concentration can help minimize the co-banding of the ER and other contaminants in the GC fractions. Although successful, the currently used sucrose concentrations (21.5 and 37%) yielded a fraction of contamination in the separated GC fraction as demonstrated by the immunoblotting. A series of different sucrose concentrations can be assayed, ranging from 21.5 to 35%, while keeping the lower-layer concentration unchanged, which would help determine the optimal sucrose concentration for crude ER banding. The second hypothesis to test is that the removal of the soluble starch fraction from the extract would improve the yield of fractionation by adjusting the medium density. The low-speed centrifugation can remove insoluble starch while the soluble fraction can be differentially precipitated with ethanol. Although membrane proteins are not known to be alcohol soluble, it is recommended to test through SDS-PAGE for any alcohol-soluble protein that may co-precipitate with starch. The third hypothesis to test in improving the sucrose-gradient fractionation is that increasing the solubility of proteins will help the band distribution in the SDS-PAGE, especially the membrane-rich enriched fractions. This can be achieved by the introduction of a detergent (0.1-1% Triton X-114, 2-4 M urea and thiourea) to improve the solubility of proteins before loading into the 1-D SDS-PAGE, especially for the enriched fractions with membrane-protein content. The fourth hypothesis is that the utilization of RNAase can help improve the yield of rough ER. Since RNA is bound to ribosome, its precipitation during centrifugation will carry the precipitation of a fraction

of the rough ER, thus decreasing its recovery. RNAse can eliminate the RNA fraction from the extract prior to the high-speed centrifugation and consequently, preserve the rough ER fraction.

B. Testing for additional enzymes markers:

The hypothesis is that testing for other contaminants in the separated fractions can confirm the success of fractions. The Western-blot immunodetection can be broadened to include analyzing the presence of enzyme markers for plastids after the two-phase partitioning. The presence of markers for ribosomes can also be tested to confirm their removal from the rough ER fraction. The enrichment of fractions can also be analyzed by the use of electron microscopy.

C. Improving the 2-D resolution:

The hypothesis is that improving the membrane solubility and sample purity from trace minerals will help resolve complex bands in 2-D electrophoresis. The improvement of the 2-D resolution can include the trial of newer commercially available kits for the sample solubilization. Other steps can include increasing the focusing time from 4 h in two hours intervals up to 18 h. Also commercially available kits can be tried to help purify the sample from trace minerals that can affect the focusing resolution.

AKNOWLEDGMENT

Special thanks to Dr. Patricia Rayas-Duarte for her technical and financial support of this project. The assistance of Department of Biochemistry and Molecular Biology at Oklahoma State University is also appreciated for the grant that helped achieving this study, and also for the Howard Hughes Medical Institute for the scholarship that helped exploring the finding of this project in a deeper manner. Appreciations are also expressed to the Food and Agriculture Product Research Center for providing financial assistance and laboratory facilities and to the Core facility Center at Oklahoma State University for providing lab equipments and technical assistance to help the accomplishment of this study.

CITED LITERATURE

1. NAAS/USDA, *National Agricultural Statistical Service/United States Department of Agriculture*. 2002. Published Estimates Data Base.

2. Berger, F. 1999. Endosperm development. *Curr. Opin. Plant Biol.,* 2, 28–32.

3. Dupont, F., and Altenbach, S. 2003. Molecular and biochemical impacts of environmental factors on wheat grain development and protein synthesis. *J. Cereal Sci.,* 38, 133-146.

4. Nehls, S., Snapp, E., Cole, N., Zaal, K., and Kenworthy, A. 2000. Dynamics and retention of misfolded proteins in native ER membranes. *Nat. Cell Biol.,* 2, 288-95.

5. DuPont, F., Hurkman, W., Tanaka, C.,and Chan, R. 1998. BiP, HSP70, NDK and PDI in wheat endosperm. I. Accumulation of mRNA and protein during grain development. *Physiol. Plant*., 103, 70-79.

6. Morré, DJ., Penel, C., Morré, DM., Sandelius, A., Moreau, P., and Anderson, B. 1991. Cell-free transfer and sorting of membrane lipids in spinach. *Protoplasma*., 160, 49-64.

7. Morré, D., and Andersson, B. 1994. Isolation of all major organelles and membranous cell components from a single homogenate of green leaves. *Meth. Enzymol*., 228, 412-419.

8. Bergstrand, A., and Dallner, G. 1969. Isolation of rough and smooth microsomes from rat liver by means of a commerically available centrifuge. *Anal. Biochem*., 29, 351-356.

9. Kreibich, G., Ulrich, B., and Sabatani, D. 1978. Proteins of rough microsomal membranes related to ribosome binding. I. Identification of ribophorins I and II, membrane proteins characteristic of rough microsomes. *J. Cell Biol*., 77, 464-487.

10. Kapoor, M., Srinivas, H., Kandiah, E., Gemma, E., Ellgaard, L., Oscarson, S., Helenius, A., and Surolia, A. 2003. Interactions of substrate with calreticulin, an endoplasmic reticulum chaperone. *J. Biol. Chem*., 278, 6194-6200.

11. Bashour, A., and Bloom, G. 1998. 58K, a microtubule-binding Golgi protein, is a formiminotransferase cyclodeaminase. *J. Biol. Chem*., 273, 19612-19617.

12. Skylas, D., Mackintosh, J., Cordwell, S., Basseal, D., Walsh, B., Harry , J., Blumenthal, C., Copeland, L., Wrigley, W., and Rathmell W. 2000. Proteome approach to the characterization of protein composition in the developing and mature wheat-grain endosperm. *J. Cereal Sci*., 32, 169–188.

13. Shevchenko, A., Wilm, M., Vorm, O., and Mann, M. 1996. Mass spectrometric sequencing of proteins from silver-stained polyacrylamide gels. *Anal. Chem*., 68, 850-858.

14. Baud S., Boutin, J., Miquel, M., Lepiniec, L., and Rochat, C. 2002. An integrated overview of seed development in Arabidopsis thaliana ecotype. *Plant Physiol. Biochem.* 40, 151-160.

15. Shimoni, Y., Segal, G., Zhu, X., and Galili G. 1995. Nucleotide sequence of a wheat cDNA encoding protein disulfide isomerase *Plant Physiol.,* 107, 281-281.

16. Chaumont, F., Barrieu, F., Wojcik, E., Chrispeels, M., and Jung R. 2001. Aquaporins constitute a large and highly divergent protein family in maize. *Plant Physiol.,* 125, 1206-1215

17. Sanchez-Barrena, M., Martinez-Ripoll, M., Zhu J., and Albert A. 2005. The Structure of the *Arabidopsis thaliana* SOS3: Molecular Mechanism of Sensing Calcium for Salt Stress Response. *J Mol Biol.,* 345, 1253-64.

18. Soni R., Carmichael J., Shah Z., and Murray J. 1995. A family of cyclin D homologs from plants differentially controlled by growth regulators and containing the conserved retinoblastoma protein interaction motif. *Plant Cell,* 7, 85-103

19. Koike M., Okamoto T., Tsuda S., and Imai R. 2002. A novel plant defensin-like gene of winter wheat is specifically induced during cold acclimation. *Biochem. Biophys. Res. Commun.,* 298, 46-53.

20. Hellen C., Facke, M., Krausslich, H., Lee, C., and Wimmer, E. 1991. Characterization of poliovirus 2A proteinase by mutational analysis: residues required for autocatalytic activity are essential for induction of cleavage of eukaryotic initiation factor 4F polypeptide p220. *J Virol.,* 65, 4226-4231.

21. Li, Z., Mouille, G., Kosar-Hashemi, B., Rahman, S., Clarke, B., Gale, K., Appels, R., and Morell, M. 2000. The structure and expression of the wheat starch synthase III gene. Motifs in the expressed gene define the lineage of the starch synthase III gene family. *Plant Physiol.,* 123, 613-624.

22. Jiang, H., Dian, W., Liu, F., and Wu, P. 2003. Cloning and characterization of a glucose 6-phosphate/phosphate translocator from Oryza sativa. *J Zhejiang Univ. Sci*., 4, 331-335.

23. Ishida A, Tada Y, Nimura T, Sueyoshi N, Katoh T, Takeuchi M, Fujisawa H, Taniguchi T, and Kameshita I. 2005. Identification of major Ca (2+)/calmodulin-dependent protein kinase phosphatase-binding proteins in brain: biochemical analysis of the interaction. *Arch. Biochem. Biophys.,* 435, 134-146.

24. Browning, K., Webster, C., Roberts, J., and Ravel, J. 1992. Identification of an isozyme form of protein synthesis initiation factor 4F in plants. *J Biol. Chem.,* 267, 10096-10100

25. Blecher, O., Erel, N., Callebaut, I., Aviezer, K., and Breiman, A. 1996. A novel plant peptidyl-prolyl-cis-trans-isomerase (PPIase): cDNA cloning, structural analysis, enzymic activity and expression. *Plant Mol. Biol.,* 32, 493-504

26. Cabello-Hurtado, F., Zimmerlin, A., Rahier, A., Taton, M., Derose, R., Nedelkina, S., Batard, Y., Durst, F., Pallett, K., and Werck-Reichhart D. 1997. Cloning and functional expression in yeast of a cDNA coding for an obtusifoliol 14alpha-demethylase (CYP51) in wheat. *Biochem. Biophys. Res. Commun.,* 230, 381-385.

27. Thain, S., Murtas, G., Lynn, J., McGrath R., and Millar, A. 2002. The circadian clock that controls gene expression in Arabidopsis is tissue specific. *Plant Physiol.,* 130, 102-110.

28. Chaumont, F., Barrieu, F., Wojcik, E., Chrispeels, M., and Jung, R. 2001. Aquaporins constitute a large and highly divergent protein family in maize. *Plant Physiol*., 125, 1206-1215.

29. Bruchhaus, I., Roeder, T., Lotter, H., Schwerdtfeger, M., and Tannich, E. 2002. Differential gene expression in Entamoeba histolytica isolated from amoebic liver abscess. *Mol. Microbiol*., 44, 1063-1072.

31. Sasaki, T., Matsumoto, T., Yamamoto, K., Sakata, K., Baba, T., Katayose, Y., Wu, J., Niimura, Y., Cheng, Z., Nagamura, Y., Antonio, B., Kanamori, H., Hosokawa, S., Masukawa, M., Arikawa, K., Chiden, Y., Hayashi, M., Okamoto, M., Ando T., and Gojobori, T. 2002. The genome sequence and structure of rice chromosome 1. *Nature,* 420, 312-316.

30. Carpi, A., Di Maira, G., Vedovato, M., Rossi, V., Naccari, T., Floriduz, M., Terzi, M., and Filippini, F. 2002. Comparative proteome bioinformatics: Identification of a whole complement of putative protein tyrosine kinases in the model flowering plant Arabidopsis thaliana. *Proteomics,* 11, 1494-1503.

32. Swarbreck, D., Ripoll, P., Brown, D., Edwards, K., and Theodoulou, F. 2003. Isolation and characterization of two multidrug resistance associated protein genes from maize. *Gene,* 315, 153-64.

33. Lawton, M., Yamamoto, R., Hanks, S., and Lamb, C. 1989. Molecular cloning of plant transcripts encoding protein kinase homologs. *Proc. Natl. Acad. Sci. USA*., 86, 3140-3144.

34. Liu, J., Ekramoddoullah, A., Piggott, N., and Zamani, A. 2004. Molecular cloning of a pathogen/wound-inducible PR10 promoter from Pinus monticola and characterization in transgenic Arabidopsis plants. *Planta,* Dec 18 [E-publication ahead of print].

35. Tada, F., Hatano, M.,Nakayama, Y., Volrath, S., Guyer, D., Ward, E., and Ohta D. 1995. Insect cell expression of recombinant imidazoleglycerolphosphate dehydratase of Arabidopsis and wheat and inhibition by triazole herbicides. *Plant Physiol*., 109, 153-159.

36. Pastore, D., Trono, D., Laus, M., Di Fonzo, N., and Passarella, S. 2001. Alternative oxidase in durum wheat mitochondria. Activation by pyruvate, hydroxypyruvate and glyoxylate and physiological role. *Plant Cell Physiol*., 42, 1373-82.

37. Marana, C., Garcia-Olmedo, F., and Carbonero P. 1990. Differential expression of two types of sucrose synthase-encoding genes in wheat in response to anaerobiosis, cold shock and light. *Gene,* 88, 167-172.

38. LaFayette, P., Eriksson, K., and Dean J. 1999. Characterization and heterologous expression of laccase cDNAs from xylem tissues of yellow-poplar (Liriodendron tulipifera). *Plant Mol. Biol.,* 40, 23-35.

39. Reyes, J., Hennig, L., and Gruissem, W. 2002. Chromatin-remodeling and memory factors. New regulators of plant development. *Plant Physiol.*, 130, 1090-1101.

40. Ritte, G., Lorberth, R., and Steup, M. 2000. Reversible binding of the starch-related R1 protein to the surface of transitory starch granules. *Plant J.,* 21, 387-391.

41. Molina, A., and Garcia-Olmedo, F. 1993. Developmental and pathogen-induced expression of three barley genes encoding lipid transfer proteins. *Plant J.,* 4, 983-991.

42. Leslie, E., Deeley R., and Cole. S. 2001. Toxicological relevance of the multidrug resistance protein 1, MRP1 (ABCC1) and related transporters. *Toxicology,* 167, 3-23.

43. White, A., and Metcalf, W. 2002. Isolation and biochemical characterization of hypophosphite/2-oxoglutarate dioxygenase. A novel phosphorus-oxidizing enzyme from Psuedomonas stutzeri WM88. *J Biol. Chem*., 277, 38262-38271.

44. Horn, R., and Paulsen, H. 2004. Early steps in the assembly of light-harvesting chlorophyll *a*/*b* complex: time-resolved fluorescence measurements. *J Biol Chem*., 279, 44400-44406.

45. Ochiai, Y., Itoh, K., Sakurai, E., and Tanaka, Y. 2005. Molecular cloning and characterization of rat semicarbazide-sensitive amine oxidase. *Biol. Pharm. Bull.* 28, 413-418

46. Eulgem, T., Rushton, P, Robatzek S., and Somssich I. 2000. The WRKY superfamily of plant transcription factors. *Trends Plant Sci., 5*, 199–206.

47. Buschmann, P., Vaidyanathan, R., Gassmann, W., and Schroeder, J. 2000. Enhancement of Na^+ uptake currents, time-dependent inward-rectifying K^+ channel currents, and K^+ channel transcripts by K^+ starvation in wheat root cells. *Plant Physiol.,* 122, 1387-1397.

48. Chen F., and Foolad, M. 1997. Molecular organization of a gene in barley which encodes a protein similar to aspartic protease and its specific expression in nucellar cells during degeneration. *Plant Mol Biol.*, 35, 821-831.

49. Song, L., Chen, S., and Yu, X. 2004. Molecular cloning and characterization of cDNA encoding a ubiquitin-conjugating enzyme from *Clonorchis Sinensis. Parasitol., Res.,* 94, 227-32

50. Di Cola, A., Frigerio, L., Lord, J., Ceriotti, A., and Roberts, L. 2001. Ricin A chain without its partner B chain is degraded after retrotranslocation from the endoplasmic reticulum to the cytosol in plant cells. *Proc. Natl. Acad. Sci. USA,* 98, 14726-14731.

51. Oguchi, K., Tamura K., and Takahashi H. 2004. Characterization of *Oryza sativa* telomerase reverse transcriptase and possible role of its phosphorylation in the control of telomerase activity. *Gene*, 342, 57-66.

52. Duque, P., and Chua, N. 2003. IMB1, a bromodomain protein induced during seed imbibition, regulates ABA- and phyA-mediated responses of germination in *Arabidopsis.* *Plant J,* 35, 787-799.

53. Wang, A., Xia, Q., Xie, W., Dumonceaux, T., Zou, J., Datla, R., and Selvaraj, G. 2002. Male gametophyte development in bread wheat (Triticum aestivum): molecular, cellular, and biochemical analyses of a sporophytic contribution to pollen wall ontogeny. *Plant J,* 30, 613-623.

54. Okkels, J., Jepsen, L., Honberg, L., Lehmbeck, J., Scheller, H., Brandt, P., Hoyer-Hansen, G., Stummann, B., Henningsen, K., Wettstein, D., and Moeller, B. 1988. A cDNA clone encoding a 10.8 kDa photosystem I polypeptide of barley. *FEBS,* 237, 108-112

15.

55. Abulafia, S., Devos G.D., and Breiman A. 1996. Characterization of the wheat cDNA encoding the B subunit of the mitochondrial ATP synthesis. *Isr. J Plant Sci.,* 44, 77-88.

56. Katoh, Y., Takemori, H., Min, L., Muraoka, M., Doi, J., Horike, N., and Okamoto, M. 2004. Salt-inducible kinase-1 represses cAMP response element-binding protein activity both in the nucleus and in the cytoplasm. *Eur. J Biochem*., 271, 4307-4319.

57. Nakamura, Y. 2000. Structural analysis of Arabidopsis thaliana chromosome 3. I. Sequence features of the regions of 4,504,864 bp covered by sixty P1 and TAC clones. *DNA Res.,* 7, 131-135.

58. The Rice Chromosome 10 Sequencing Consortium. 2003. In-depth view of structure, activity, and evolution of rice chromosome 10. *Science*, 300, 1566-1569.

59. Kumekawa, N., Hosouchi, T., Tsuruoka, H., and Kotani, H. 2001. The size and sequence organization of the centromeric region of Arabidopsis thaliana chromosome 4. *DNA Res.* 8, 285-290.

60. Simmonds, D., and O'Brien, T. 1981. Morphological and biochemical development of the wheat endosperm. p. 27-46. In: *Advances in Cereal Science and Technology*. Ed: Pomeranze, Y. American Association of Cereal Chemists, St. Paul, MN.

61. Hinton, R., and Mullock, B. 1994. Isolation of subcellullar fractions. p. 31-69. In: *Practical Guide to MembraneProtein Purification.* Ed: Von Jagow, G. and Schigger, H. Academic Press, San Diego.

62. Graham, M. 1997. The membranes of the secretory and exocytic pathways. p. 205-242. In: *Subcellular Fractionation : a Practical Approach* Ed: Graham, J. and Rickwood, D. IRL Press at Oxford University Press, New York. .

63. Albertsson, P., Andersson, B., Larsson, C., and Akerlund, H. 1982. Phase partition a method for purification and analysis of cell organelles and membrane vesicles. *Meth. Biochem. Anal*., 28, 115-50.

64. Sazlavsky, B. 1995. Aqueous two-phase partitioning: physical chemistry and bioanalytical applications. p 96-127. Ed: Sazlavsky, B. Marcel Dekker Inc, New York.

65. Farrant, J., Bailly, C., Leymarie, J., Hamman, B, Côme, D and Corbineau, F. 2004. Wheat seedlings as a model to understand desiccation tolerance and sensitivity. *Physiol. Plant*., 120, 563-581.

66. Aleksandrushkina, N., Zamyatnina, V., Bakeeva, L., Seredina, A., Smirnova, E., Yaguzhinsky, L., and Vanyushin, B. 2004. Apoptosis in wheat seedlings grown under normal daylight. *Biochemistry*, 69, 285-294.

67. Larkin, B., and Hurkman, W. 1978. Synthesis and deposition of zein in protein bodies of maize endosperm. *Plant Physiol.*, 62, 256-263.

68. Hermo, L., Smith, C., and Charles, E. 1998. The structure of the Golgi apparatus: a sperm's eye view in principal epithelial cells of the rat epididymis. *Histochem*. *Cell Biol.*, 109, 431-447.

69. Salazar, R., Pring, D., and Kempken, F**.** 1991. Editing of mitochondrial atp9 transcripts from two sorghum lines. *Curr Genet.,* 6, 483-486.

70. Cavdar, K., Blackburn, K., Burkhart, W., and Spremulli, L. 1999. Identification of a mammalian mitochondrial homolog of ribosomal protein S7. *Biochem. Biophys. Res. Commun.* 266, 141-146.

71. Johnson, D., Hamon, M., and Fischel-Ghodsian, N. 1998. Characterization of the human mitochondrial ribosomal S12 gene. *Genomics,* 52, 363-368

72. Kumar, R., Drouaud, J., Raynal, M., and Small, I. 1995. Characterization of the nuclear gene encoding chloroplast ribosomal protein S13 from Arabidopsis thaliana. *Curr Genet*. 4, 346-352.

73. Genchi, G., Ponzone, C., Bisaccia, F., De Santis, A., Stefanizzi, L., and Palmieri,F. 1996. Purification and characterization of the reconstitutively active adenine nucleotide carrier from maize mitochondria. *Plant Physiol.*, 112, 845-851.

74. Heins, L., Mentzel, H., Schmid, A., Benz, R., and Schmitz, U. 1994. Biochemical, molecular, and functional characterization of porin isoforms from potato mitochondria. *J Biol Chem*., 269, 26402-26410

75. Gabler, L., Herz, U., Liddell, A., Leaver, C., Schroder, W., Brennicke, A., and Grohmann, L. 1994. The 42.5 kDa subunit of the NADH: ubiquinone oxidoreductase

(complex I) in higher plants is encoded by the mitochondrial nad7 gene. *Mol. Gen. Genet*., 244, 33-40.

76. hompson, M., Jacks, C., Lenvik, T., and Gantt, S. 1992. Characterization of rps17, rpl9 and rpl15: three nucleus-encoded plastid ribosomal protein genes. *Plant Mol. Biol.,* 18, 931-944

77. Kim, W., Chung, Ji H., Back, J., Choi, J., Cha, J., Koh, Hun Y., and Han, Y. 2003. Molecular cloning and characterization of an NADPH quinone oxidoreductase from Kluyveromyces marxianus. *J Biochem. Mol. Biol.,* 36, 442-449.

78. Baier, M., and Dietz, K. 1997. The plant 2-Cys peroxiredoxin BAS1 is a nuclear-encoded chloroplast protein: its expressional regulation, phylogenetic origin, and implications for its specific physiological function in plants. *Plant J*, 12, 179-190.

79. Lawrence, S., Cline, K., and Moore, G. 1997. Chromoplast development in ripening tomato fruit: identification of cDNAs for chromoplast-targeted proteins and characterization of a cDNA encoding a plastid-localized low-molecular-weight heat shock protein. *Plant Mol. Biol*., 33, 483-492.

80. Joyard, J., Block, M., Coves, J., Alban, C., and Douce, R. 1987. Characterization of plastid polypeptides from the outer and inner envelope membranes. *Met. Enzymol.,* 148, 206-218.

81. Meyer, H., Thienel, U., and Piechulla, B. 1989. Molecular characterization of the diurnal/circadian expression of the chlorophyll a/b-binding proteins in leaves of tomato and other dicotyledonous and monocotyledonous plant species. *Planta*, 180, 5-15.

82. Sugihara, K., Hanagata, N., Dubinsky, Z., Baba, S., and Karube, I. 2000. Molecular characterization of cDNA encoding oxygen evolving enhancer protein 1 increased by salt treatment in the mangrove Bruguiera gymnorrhiza. *Plant Cell Physiol*., 41, 1279-1285.

83. Ogihara, Y., Endo, A., Kojima, T., Isono, K., Hanaoka, M., Shiina, T., Terachi, T., Utsugi, S., Murata, M., Mori, N., Takumi, S., Ikeo, K., Gojobori, T., Murai, R., Murai, K., Matsuoka, Y., Ohnishi, Y., Tajiri, H., and Tsunewaki, K. 2000. Chinese spring wheat (Triticum aestivum) chloroplast genome: complete sequence and contig clones. *Plant Mol. Biol. Rep.*, 18, 243-253.

84. Lippincott-Schwartz, J., Roberts, T., and Hirschberg, K. 2000. Secretory protein trafficking and organelle dynamics in living cells. *Ann. Rev. Cell Develop. Biol.*, 16, 557-589.

85. Hirosawa, M., Nagase, T., Ishikawa, K., Kikuno, R., Nomura, N., and Ohara, O. 1999. DNA Characterization of cDNA clones selected by the GeneMark analysis from size-fractionated cDNA libraries from human brain. *DNA Res*., 6, 329-336.

86. Strausberg, R. 2002. Generation and initial analysis of more than 15,000 full-length human and mouse cDNA sequences. *Proc. Nat Acad. Sci*., 99, 16899-16903.

87. Boman, A., Zhang, C., Zhu, X., and Kahn R. 2000. A Family of ADP-Ribosylation Factor Effectors That Can Alter Membrane Transport through the *trans*-Golgi. *Mol. Biol. Cell*, 11, 1241–1255.

88. Yadav, N., Wierzbicki, A., Aegerter, M., Caster, C., Perez-Grau, L., J. Kinney, A., Hitz, W., Booth, J., Schweiger, B., Stecca, K., Allen, S., Blackwell, M., Reiter, R., Carlson, T., Russell, S., Feldmann, K., Pierce, J., and Browse, J. 1993. Cloning of higher plant [omega]-3 fatty acid desaturases. *Plant Physiol*., 103, 467-476.

89. Keon, J., Jewitt, S., and Hargreaves. J. 1995. A gene encoding γ-adaptin is required for apical extension growth in *Ustilago maydis Gene,* 162, 141-145.

90. Cortes, J., Katoh-Fukui, R., Moto, K., Ribas, J, and Ishiguro J., 2004. *Schizosaccharomyces pombe* Pmr1p Is essential for cell Wall integrity and is required for polarized cell growth and cytokinesis. *Eukaryot. Cell,* 3, 1124-1135.

91. Sood, R., Porter, A., Ma, K., Quilliam, L., and Wek, R. 2000. Pancreatic eukaryotic initiation factor-2a kinase (PEK) homologues in humans, *Drosophila melanogaster* and *Caenorhabditis elegans* that mediate translational control in response to endoplasmic reticulum stress. *Biochem. J,* 346, 281–293

92. Hwang, I., Ratterman, D., and Sze, H. 1997. Distinction between endoplasmic reticulum-type and plasma membrane-type Ca2+ pumps. Partial purification of a 120-kilodalton Ca2+-ATPase from endomembranes. *Plant Physiol.,* 113, 535-548.

93. The institute for genomic research and Kazusa DNA reseach institute. 2000. Sequence and analysis of chromosome 3 of the plant *Arabidopsis thaliana* European Union 3 Arabidopsis genome sequencing consortium. *Nature,* 408, 820-822.

94. Nakai, M., Takada T., and Endo, T. 1993. Cloning of the *YAP19* gene encoding a putative yeast homolog of AP19, the mammalian small chain of the clathrin-assembly proteins *Biochim. Biophys. Acta* 1174, 282-284.

95. Adessi, E., Miege, C., Albrieux, C., and Rabilloud, T. 1997. Two-dimensional electrophoresis of membranes proteins, A current challenge for immobilized pH gradients. *Electrophoresis* 18, 127-135.

96. Rabilloud, T., and Chevallet, M. 2000. Solubilization of proteins in two-dimensional electrophoresis. p. 9-29. In: *Proteom Reseach: Two Dimensional Gel Electrophoresis and Identification Methods.* Ed: Rabolloud T. Springer Verlag, Berlin Heiddelberg, Germany.

97. Ferrari, D. and Soling, H. 1999. The protein disulphide-isomerase family: unraveling a string of folds. *Biochem. J.* 339, 1–10.

98. Edwards, A., Marshall, J., Sidebottom, C., Visser, R., Smith, A., and Martin, C. 1995 Biochemical and molecular characterization of a novel starch synthase from potato tubers *Plant J,* 8, 283-294.

99. Chen, F., and Foolad, R. 1997. Molecular organization of a gene in barley which encodes a protein similar to aspartic protease and its specific expression in nucellar cells during degeneration. *Plant Mol. Biol.,* 35**:** 821–831.

APPENDICES

APPENDICE A: TABLES

Table 1.

Protein recovery of endoplasmic reticulum (ER) and Golgi complex (GC) enrichment from developing wheat endosperm between 7 and 60 days after anthesis (DAA).

Sample	Protein Concentration (mg/ml)				Recovery Rate (% of Cr EX)				Reduction Folds of Protein Content from CR EX			
DAA [a]	7	**14**	**34**	**60**	7	**14**	**34**	**60**	7	**14**	**34**	**60**
Cr EX [b]	53.4	69.6	101.4	113.0	100	100	100	100	0	0	0	0
Cr ER [c]	10.2	16.9	29.2	23.4	19.1	24.3	28.8	20.7	5.24	4.12	3.47	4.83
Cr GC [d]	6.4	10.4	19.1	17.6	12.0	14.9	18.8	15.6	8.34	6.69	5.31	6.42
En Er [e]	0.1	3.3	4.2	1.2	1.9	4.7	4.2	1.1	534	21.1	24.1	94.2
En GC [f]	0.5	1.2	1.6	0.7	0.9	1.7	1.6	0.6	106.8	58	63.4	161.4

[a] DAA = days after anthesis

[b] Cr EX = crude extract

[c] Cr ER = crude endoplasmic reticulum

[d] Cr GC = crude Golgi complex

[e] En ER = enriched endoplasmic reticulum

[f] En GC = enriched Golgi complex

Table 2.

Results of database search of protein spots identified by MALDI-TOF from wheat endosperm organelles during development. Spot number refers to the spot position as shown on the 2-D gels. Accession number refers to the nucleotide identification number determined by the MS-FIT search against the Unigen database for nucleotide from NCBI, and matched to protein sequence through Blast X search. The MOWSE score rank matches between theoretical fingerprints and experimental data molecular weight of peptides. Hit is an index number for matching database entries. No hits refers to no matching protein through Blast X. Spots showing a MOWSE score and hit number of 0 were not identified by MS-FIT search.

Endoplasmic Reticulum at 7 DAA No of identified spots: 7/16

Spot No.	Access No	MOWSE	Hit #	Protein description
3	13925727	9.75E+02	7/20	Protein disulfide isomerase 3 precursor [Triticum aestivum]
4	25199000	4.35E+02	4/20	No hits
7	32683037	9.21E+02	4/20	Similar to transcription factor TFIIIA [Oryza sativa]
9	25230592	1.01E+02	4/20	NOD26-like membrane integral protein ZmNIP2-1 [Zea mays]
11	39573043	1.26E+03	4/20	Putative salt tolerance protein 5 [Oryza sativa (japonica cultivar-group)]
12	14315129	3.38E+02	4/20	Unknown protein [Oryza sativa (japonica cultivar-group)]
13	32128969	2.12E+03	4/20	Cyclin A2 [Lycopersicon esculentum]

Endoplasmic Reticulum 14 DAA No of identified spots: 10/19

Spot No.	Access No	MOWSE	Hit #	Protein description
1	0	0	0	
2	32128482	2.61E+02	4/20	Defensin [Triticum aestivum]
3	55685505	1.18E+02	4/20	Putative eukaryotic translation initiation factor 2A [Oryza sativa (japonica cultivar-group)]
4	55686524	1.91E+03	4/20	No hits
6	55677838	1.91E+03	4/20	No hits
7	20106055	1.46E+02	5/20	OSJNBa0033H08.12 [Oryza sativa (japonica cultivar-group)]
9	9502142	9.98E+01	4/20	Starch synthase III [Triticum aestivum]
10	25204051	4.10E+01	4/20	Phosphate translocator-like [Oryza sativa (japonica cultivar-group)]
18	32128860	1.74E+02	4/20	Putative calcium/calmodulin-dependent protein kinase CaMK [Oryza sativa (japonica cultivar-group)]
19	55609305	9.19E+01	4/20	OSJNBa0071I13.18 [Oryza sativa (japonica cultivar-group)]

Endoplasmic Reticulum 34 DAA No of identified spots: 6/19

Spot No.	Access No	MOWSE	Hit #	Protein description
7	452439	4.02E+02	4/20	Eukaryotic initiation factor (iso)4F subunit p82-34 (eIF-(iso)4F p82-34)
10	854625	1.38E+01	4/20	Peptidylprolyl isomerase [Triticum aestivum]
11	20332776	2.80E+02	4/20	No Hits
13	0	0.00E+00	0	
16	32554747	4.98E+01	4/20	No hits
18	32129002	5.00+E03	4/20	NBS-LRR-like protein [Oryza sativa (japonica cultivar-group)]

Endoplasmic Reticulum DAA60 No of identified spots: 14/39

Spot No.	Access No	MOWSE	Hit #	Protein description
1	25158654	1.18E+03	4/20	No hits
2	25210110	1.18E+04	4/20	Cytochrome P450 [Lotus corniculatus var. japonicus]
13	39556126	1.36E+06	4/20	Putative timing of CAB expression 1 [Oryza sativa (japonica cultivar-group)]
14	25243299	1.98E+04	5/20	No hits
15	38970673	6.67E+03	4/20	Unknown protein [Oryza sativa (japonica cultivar-group)]
19	32549375	6.31E+03	4/20	Plasma membrane integral protein ZmPIP2-6 [Zea mays]
21	38975796	1.94E+03	5/20	Putative GTP-binding protein RAB7D [Arabidopsis thaliana]
26	31418039	2.03E+04	5/20	No hits
27	21483048	4.77E+02	4/20	Putative protein tyrosine-serine-threonine kinase [Oryza sativa (japonica cultivar-group)]
29	0	0.00E+00	0	No hits
30	55680897	7.40E+02	4/20	Putative disease resistance protein [Oryza sativa (japonica cultivar-group)]
31	39619660	1.28E+02	4/20	Putative DNA-directed RNA polymerase II 13.6K chain [Oryza sativa (japonica cultivar-group)]
32	39573038	5.03E+02	4/20	No hits
34	19957420	1.12E+03	4/20	Putative multidrug-resistance associated protein [Oryza sativa (japonica cultivar-group)]

Golgi Complex 7 DAA No of identified spots:3/9

Spot No.	Access No	MOWSE	Hit #	Protein description
5	31369559	1.71E+03	4/20	putative serine/threonine protein kinase [Oryza sativa (japonica cultivar-group)]
6	39622081	1.29E+03	4/20	putative wound inducive protein [Oryza sativa (japonica cultivar-group)]
7	0	0.00+00	0	

Golgi Complex 14 DAA. No of identified spots:16/40

Spot No.	Access No	MOWSE	Hit #	Protein description
1	55675504	1.40E+02	4/20	No hits
2	437214	2.68E+03	5/20	Imidazoleglycerolphosphate dehydratase [Arabidopsis Thaliana]
8	19912726	1.09E+03	4/20	Alternative oxidase [Triticum aestivum]
10	3393043	2.61E+02	6/20	Sucrose synthase type 2 [Triticum aestivum]
15	25418342	5.70E+01	4/20	No hits
18	32690206	4.88E+02	4/20	No hits
22	25163221	3.32E+02	4/20	Laccase [Liriodendron tulipifera]
23	39573401	4.58E+01	4/20	Putative nucleosome/chromatin assembly factor A [Oryza sativa (japonica cultivar-group)]
24	20549754	2.03E+02	4/20	Starch associated protein R1 [Solanum tuberosum]
29	0	0.00E+00	0	
30	39003585	5.25E+02	4/20	Ow-21 peptide,non specific lipid transfer protein [Hordeum vulgare subsp. vulgare]
31	0	0.00E+00	0	
32	13925725	2.29E+02	5/20	Protein disulfide isomerase 2 precursor [Triticum aestivum]
35	33329358	3.83E+00	4/20	Multidrug resistance associated protein MRP2 [Triticum aestivum]
37	55608969	6.24E+02	5/20	Putative 2-oxoglutarate-dependent dioxygenase [Oryza sativa (japonica cultivar-group)]
38	39003566	1.11E+03	4/20	Chlorophyll a/b-binding protein WCAB precursor [Triticum aestivum]

Golgi Complex 34 DAA No of identified spots: 19/63

Spot No.	Access No	MOWSE	Hit #	Protein description
7	9608785	6.17E+01	4/20	OSJNBb0103D08.7 [Oryza sativa (japonica cultivar-group)]
8	24979931	1.91E+02	4/20	Unknown protein [Oryza sativa (japonica cultivar-group)]
14	0	0.00E+00	0	No hits
15	32558911	1.02E+03	4/20	OSJNBa0064G10.8 [Oryza sativa (japonica cultivar-group)]
16	0	0.00E+00	0	No hits
17	24992242	2.75E+02	4/20	No hits
18	55606686	3.69E+02	4/20	No hits
19	31157877	6.46E+03	4/20	Amine oxidase-related [Arabidopsis thaliana]
20	38990771	4.81E+01	4/20	Putative WRKY DNA binding protein [Oryza sativa (japonica cultivar-group)]
21	39618085	1.00E+03	4/20	OSJNBa0023J03.8 [Oryza sativa (japonica cultivar-group)]
23	39566907	1.85E+00	4/20	Putative AKT1-like potassium channel [Hordeum vulgare]
24	39617784	3.36E+03	4/20	Nucellin-like aspartic protease [Zea mays]
25	39569130	3.68E+02	4/20	Putative ubiquitin-conjugating enzyme E2 [Oryza sativa (japonica cultivar-group)]
26	39573157	6.01E+04	4/16	Proteasome inhibitor-like protein [Oryza sativa (japonica cultivar-group)]
49	25243299	4.94E+03	4/17	No hits
52	0	0.00E+00	0	No hits
54	14315395	6.38E+02	4/20	No hits
55	39559339	3.70E+02	4/20	Putative protein kinase [Oryza sativa]
56	25241866	2.68E+02	4/20	Putative seed imbibition protein [Oryza sativa (japonica cultivar-group)]

GC 60. No of identified spots: 10/29

Spot No.	Access No	MOWSE	Hit #	Protein description
1	22003085	2.29E+02	8/20	Fatty acyl coA reductase [Triticum aestivum]
2	39617332	1.15E+03	4/20	Photosystem I reaction center subunit IV, chloroplast precursor (PSI-E) (Photosystem I 10.8 kDa polypeptide)
4	38992468	1.04E+03	4/20	Protein disulfide isomerase [Zea mays]
15	25257233	7.50E+02	4/20	No hits
18	525290	2.21E+07	12/20	ATP synthase beta subunit [Triticum aestivum]
18	55674091	2.60E+04	5/20	Salt-inducible protein kinase [Zea mays]
20	39571762	6.41E+02	4/20	Chloroplast nucleoid DNA-binding protein -like protein [Oryza sativa (japonica cultivar-group)]
21	55674091	5.75E+03	4/20	Salt-inducible protein kinase [Zea mays]
28	39567990	4.23E+02	4/20	Putative transcription initiation factor [Oryza sativa (japonica cultivar-group)]
29	32549354	9.23E+03	4/20	AP2 domain transcription factor EREBP [Oryza sativa (japonica cultivar-group)]

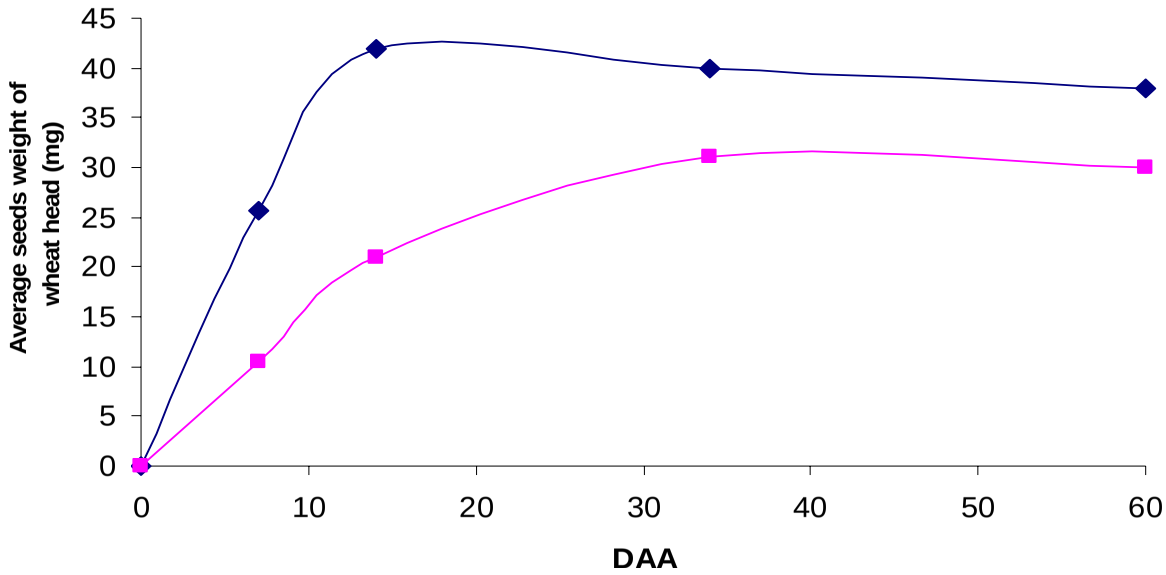

Fig: 1. Pattern of weight change of wheat endosperm during development analyzed at 4 stages of growth: 7, 14, 43, and 60 days after anthesis (DAA). (♦) is the change of fresh weight; (■) is the change on dry weight. Each point represents the average weight of seeds in three wheat heads. The x-axis represents the time point of development. The y-axis represents the average weight of one seeds.

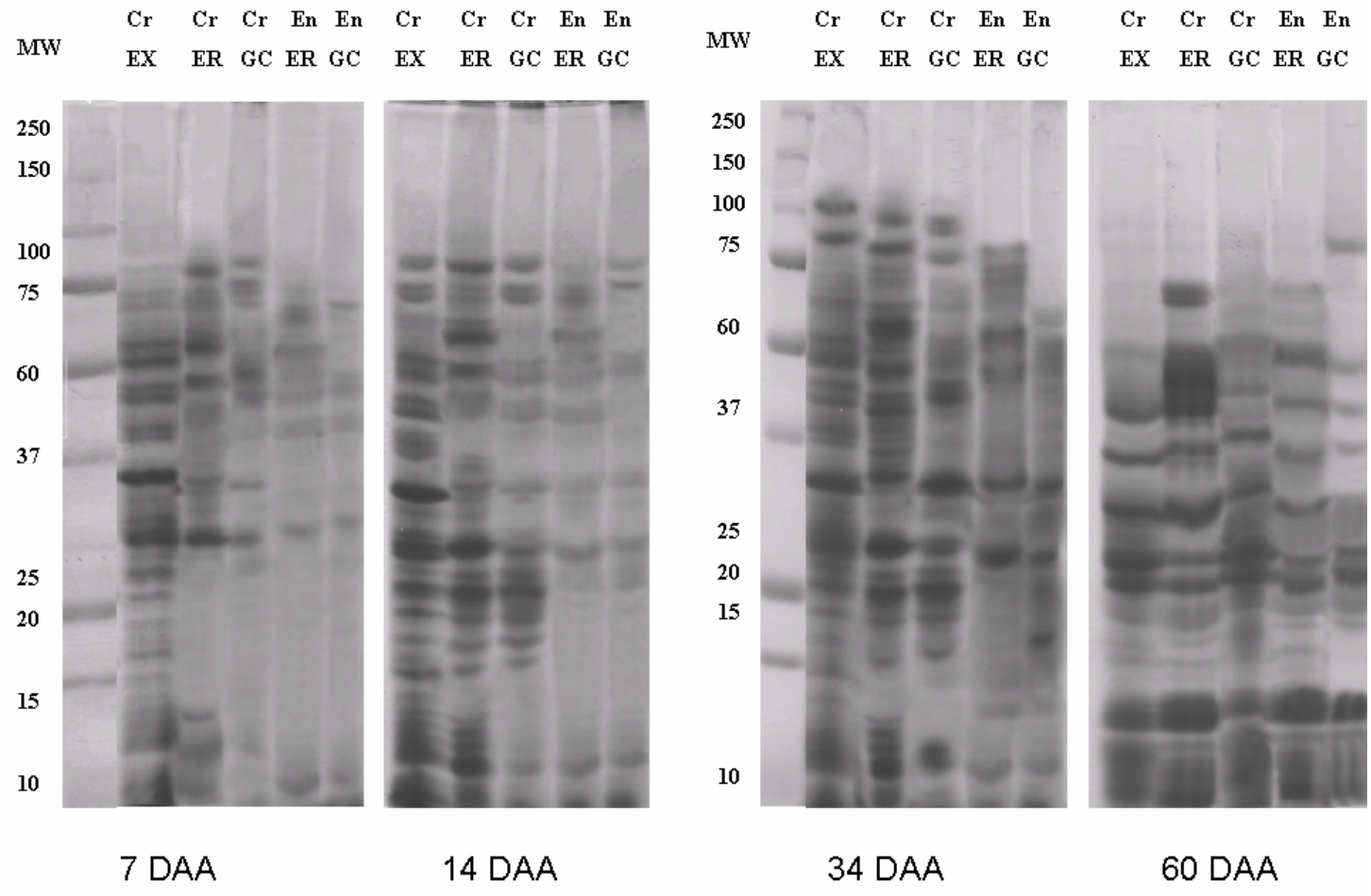

Fig 2: SDS-PAGE showing the pattern of organelles enrichment at the 4 stages of wheat development. Cr Ex: crude extract obtained by low speed centrifugation (1000 x g). Cr ER: crude endoplasmic reticulum. Cr GC: crude Golgi complex. Both fractions were obtained by high speed centrifugation (65,000 x g). En ER: enriched endoplasmic reticulum obtained by two phase partitioning and removal of ribosome bound. En GC:

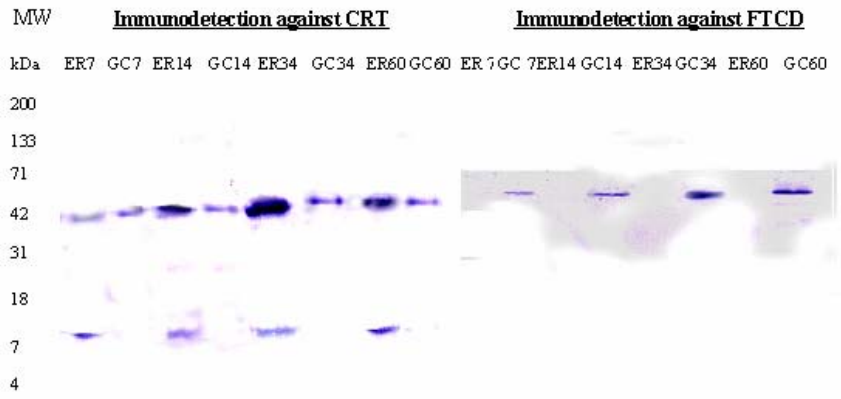

Fig. 3: Western blot analysis of endoplasmic reticulum (ER) and the Golgi complex (GC) enrichment extract from developing wheat endosperm between 7 and 60 days after anthesis. 15 µl of extracted were loaded in each well.
CRT = calreticulin, an ER enzyme marker
FTCD = formiminotransamidase cyclodiaminase, a GC enzyme marker.
MW=molecular weight for marker (kDa).
ER 7: endoplasmic reticulum obtained at 7 DAA (days after anthesis)
GC 7: Golgi complex obtained at 7 DAA
ER 14: endoplasmic reticulum obtained at 14 DAA
GC 14: Golgi complex obtained at 14 DAA
ER 34: endoplasmic reticulum obtained at 34 DAA
GC 34: Golgi complex obtained at 34 DAA
ER 60: endoplasmic reticulum obtained at 60 DAA
GC 60 Golgi complex obtained at 60 DAA

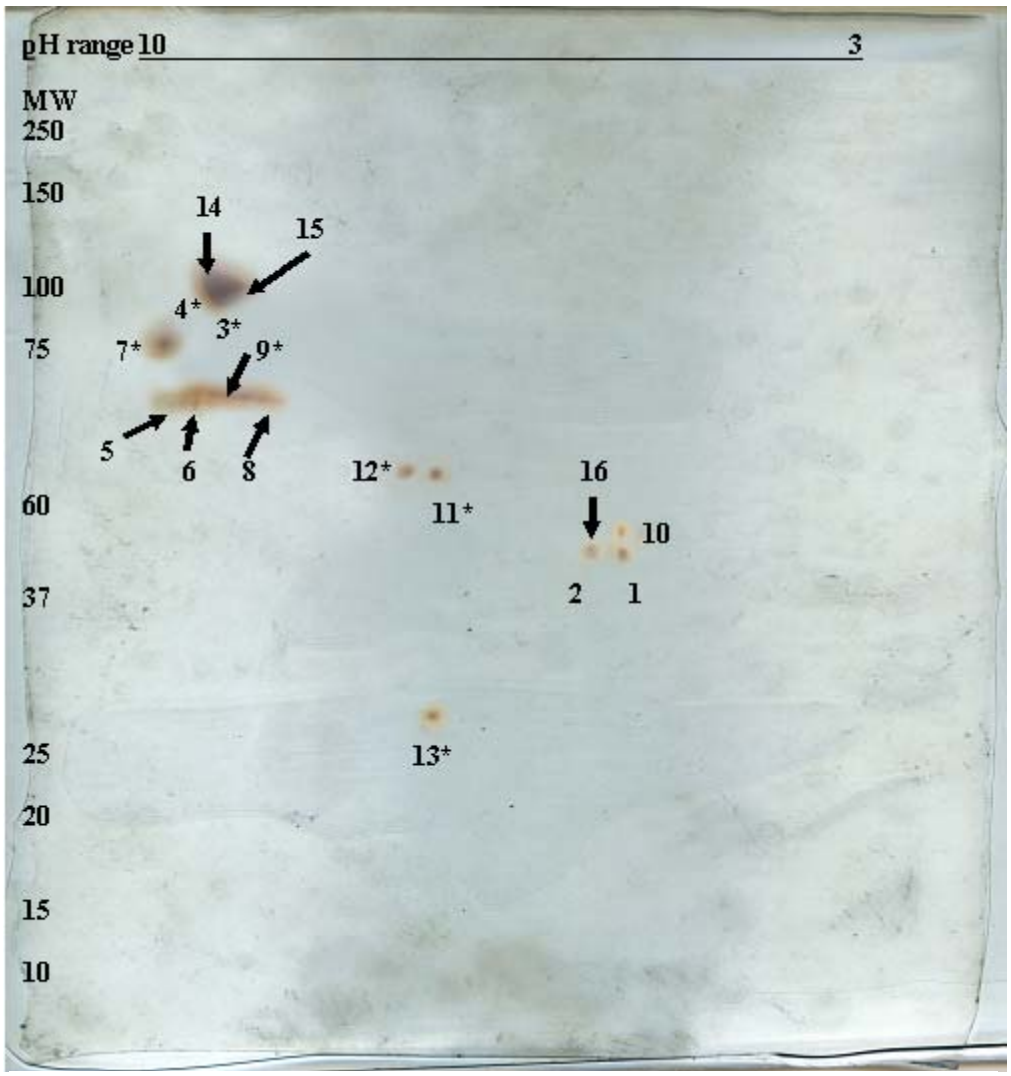

Fig 4-1: 2-D separation of enriched ER fraction at 7 DAA: No of identified samples: 7/16. Numbers followed by asterisks represents proteins identified by MALDI-TOF.

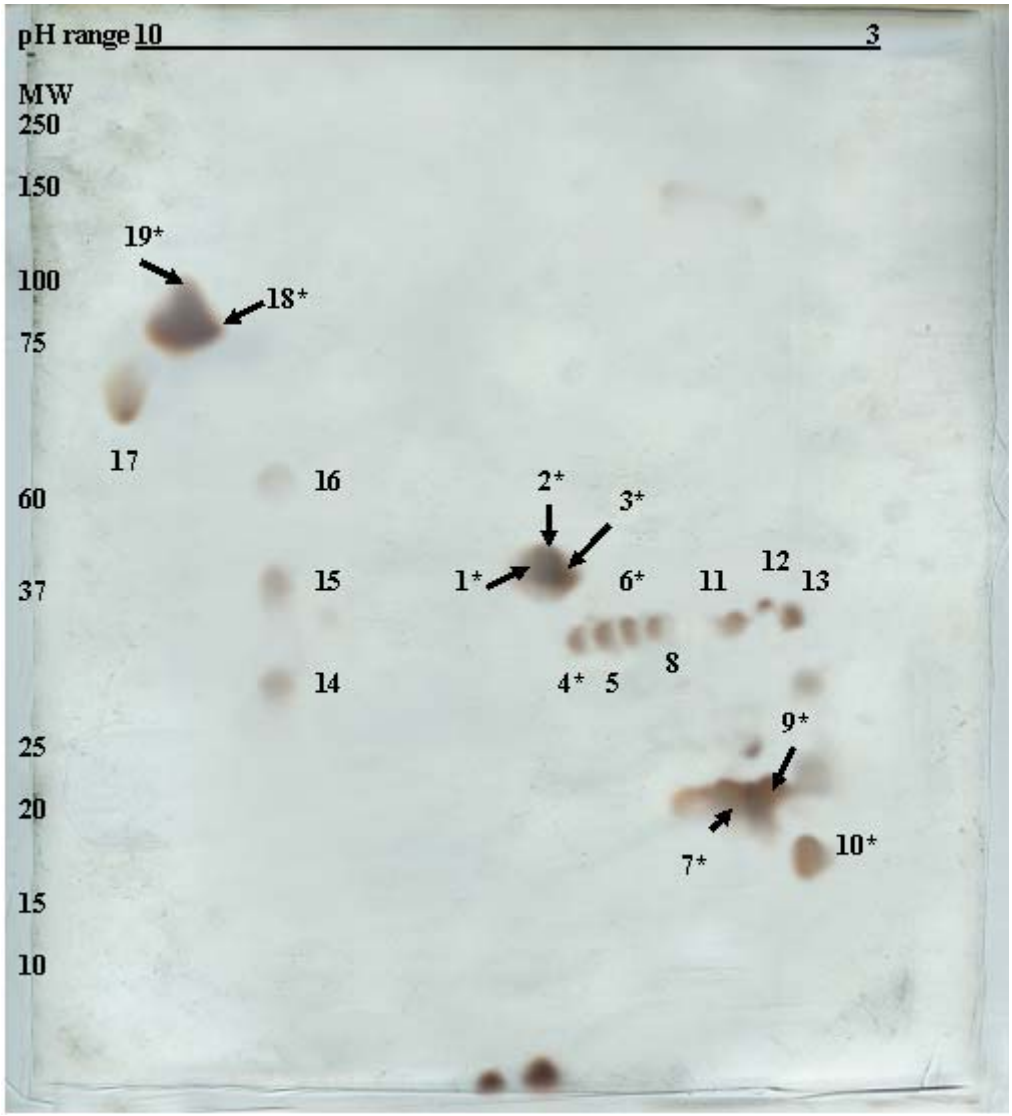

Fig 4-2: 2-D separation of enriched ER fraction at 14 DAA. No of identified samples: 6/19. Numbers followed by asterisks represents proteins identified by MALDI-TOF.

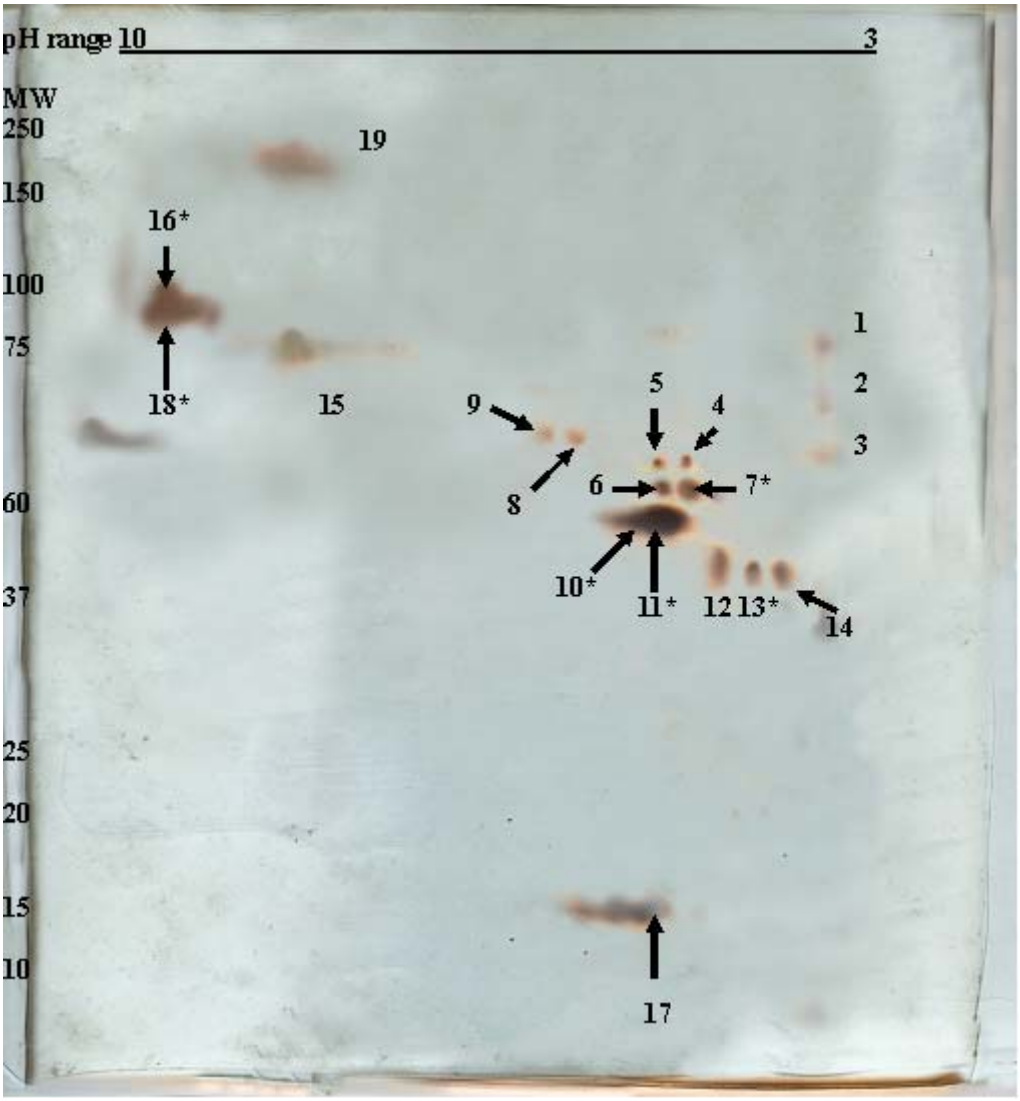

Fig 4-3: 2-D separation of enriched ER fraction at 34 DAA: No of identified samples: 6/19. Numbers followed by asterisks represents proteins identified by MALDI-TOF.

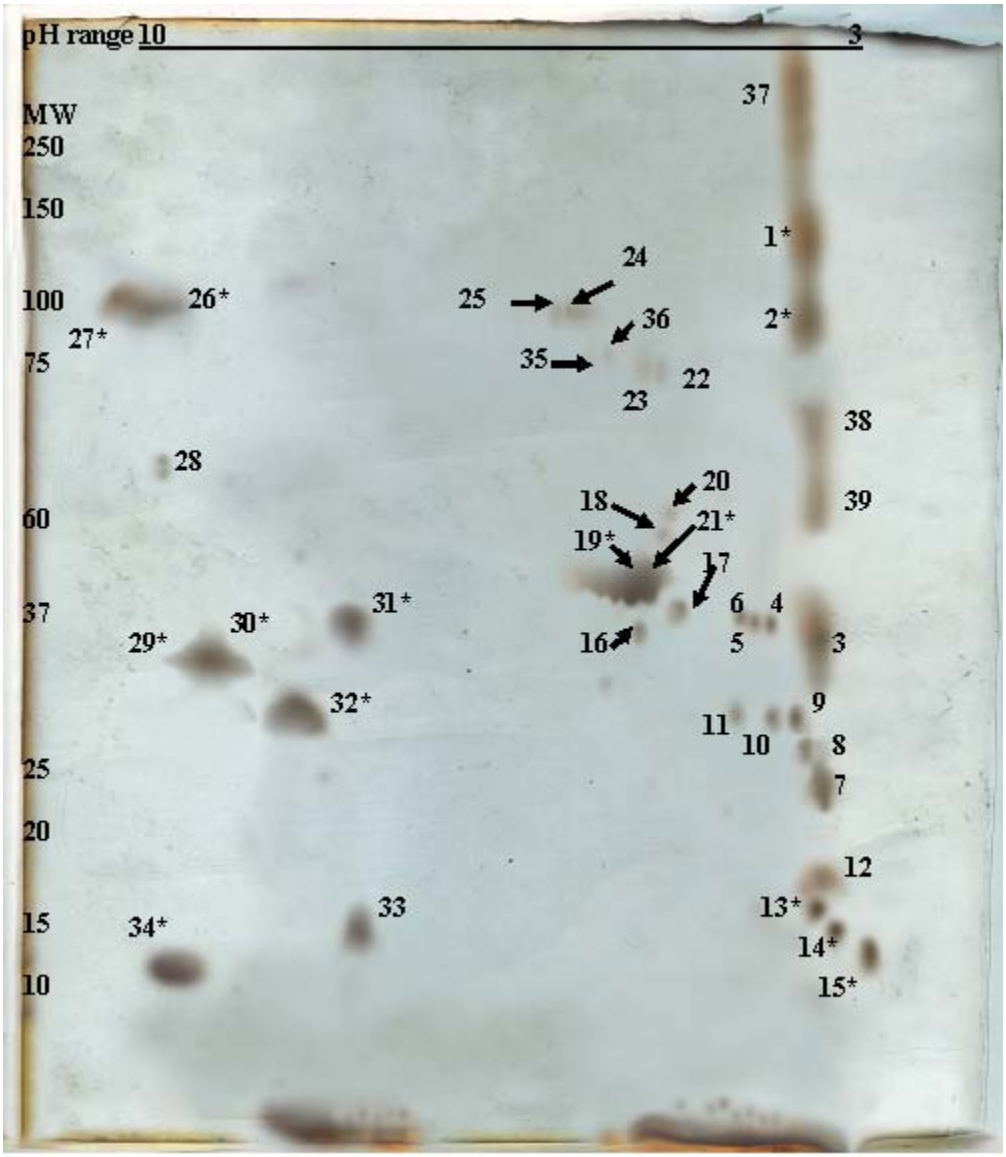

Fig 4-4: 2-D separation of enriched ER fraction at 60 DAA. No of identified spots: 14/39. Numbers followed by asterisks represents proteins identified by MALDI-TOF.

Fig 4-5: 2-D separation of enriched GC fraction at 7 DAA: No of identified samples:3/9 Numbers followed by asterisks represents proteins identified by MALDI-TOF.

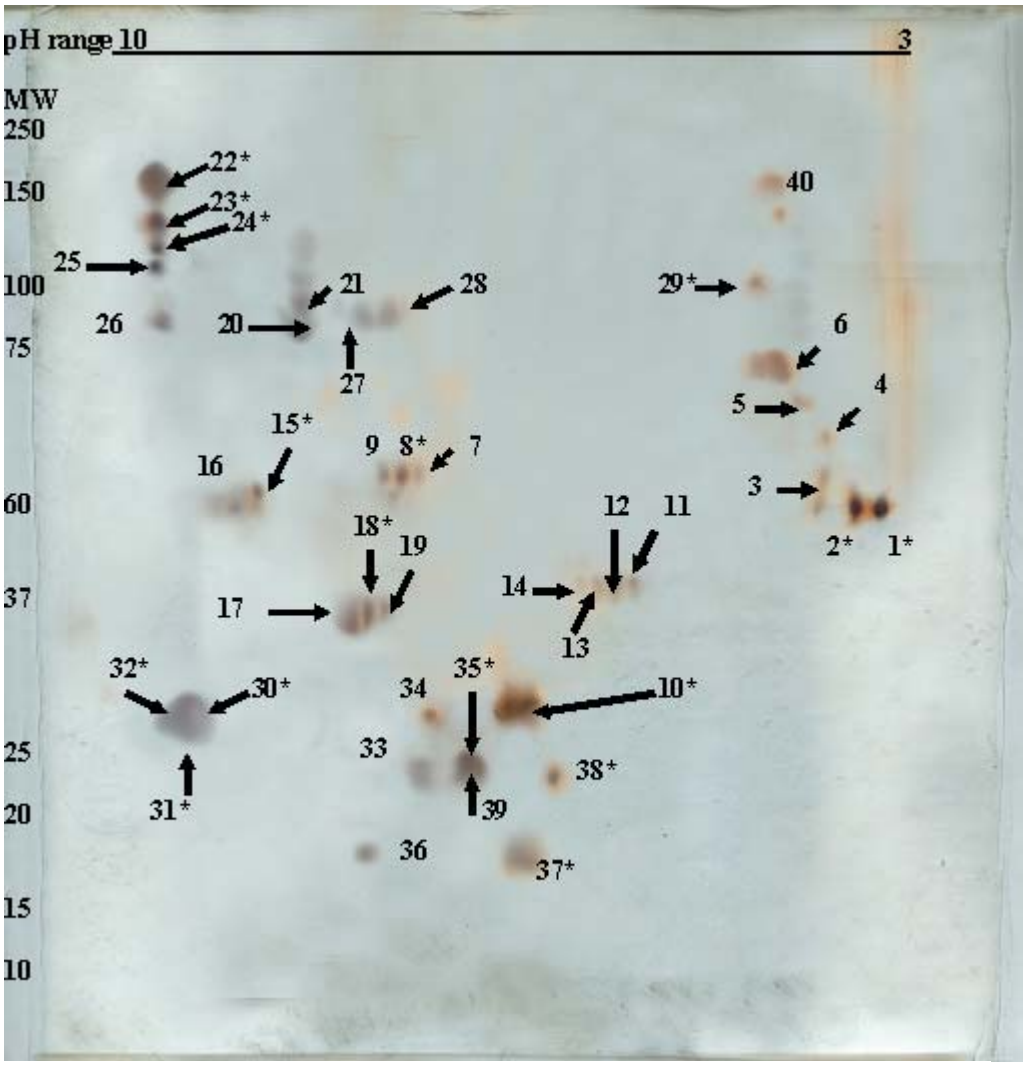

Fig 4-6: 2-D separation of enriched GC fraction at 14 DAA. No of identified samples: 16/40. Numbers followed by asterisks represents proteins identified by MALDI-TOF.

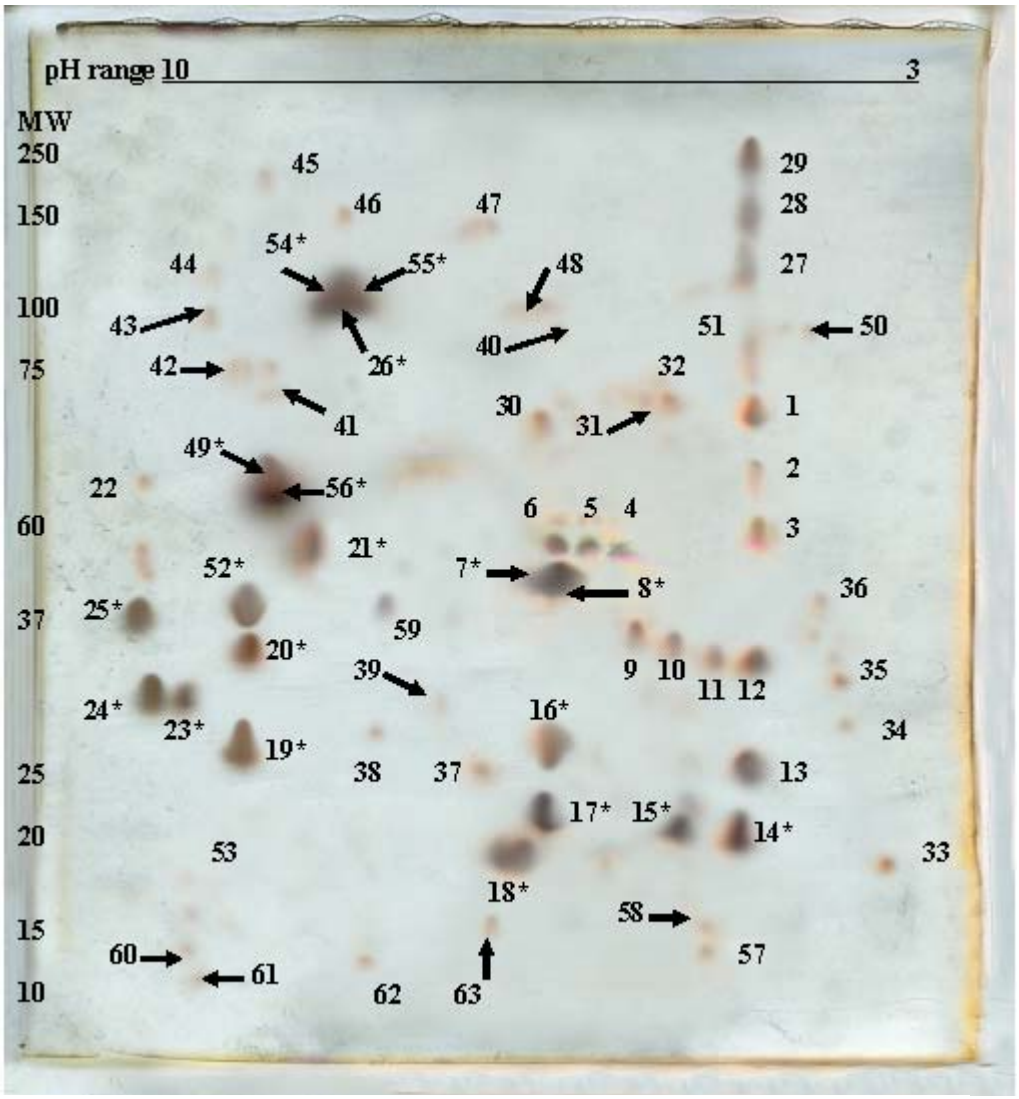

Fig 4-7: 2-D separation of enriched GC fraction at 34 DAA. No of identified samples: 19/63. Numbers followed by asterisks represents proteins identified by MALDI-TOF.

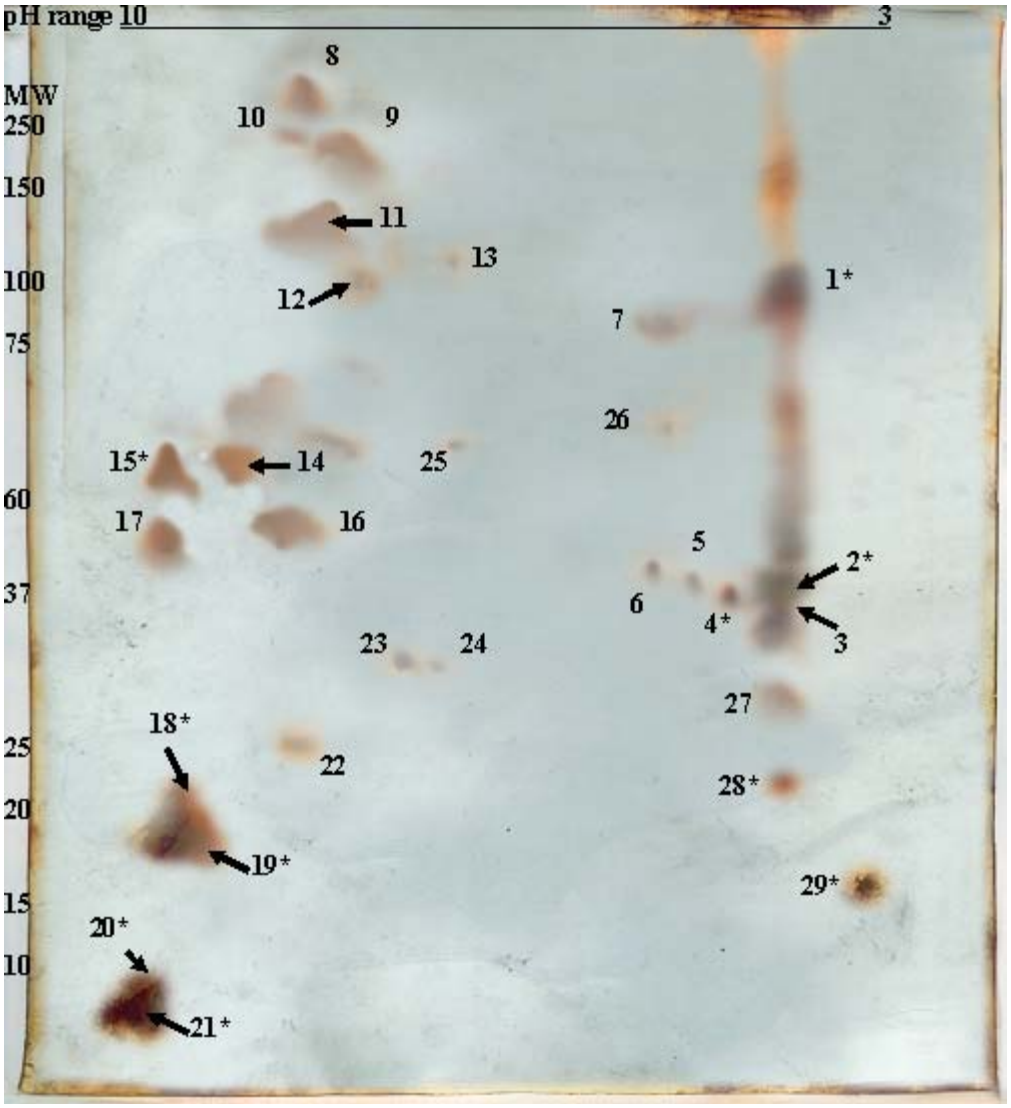

Fig 4-8: 2-D separation of enriched GC fraction at 60 DAA: No of identified spots: 10/29. Numbers followed by asterisks represents proteins identified by MALDI-TOF.

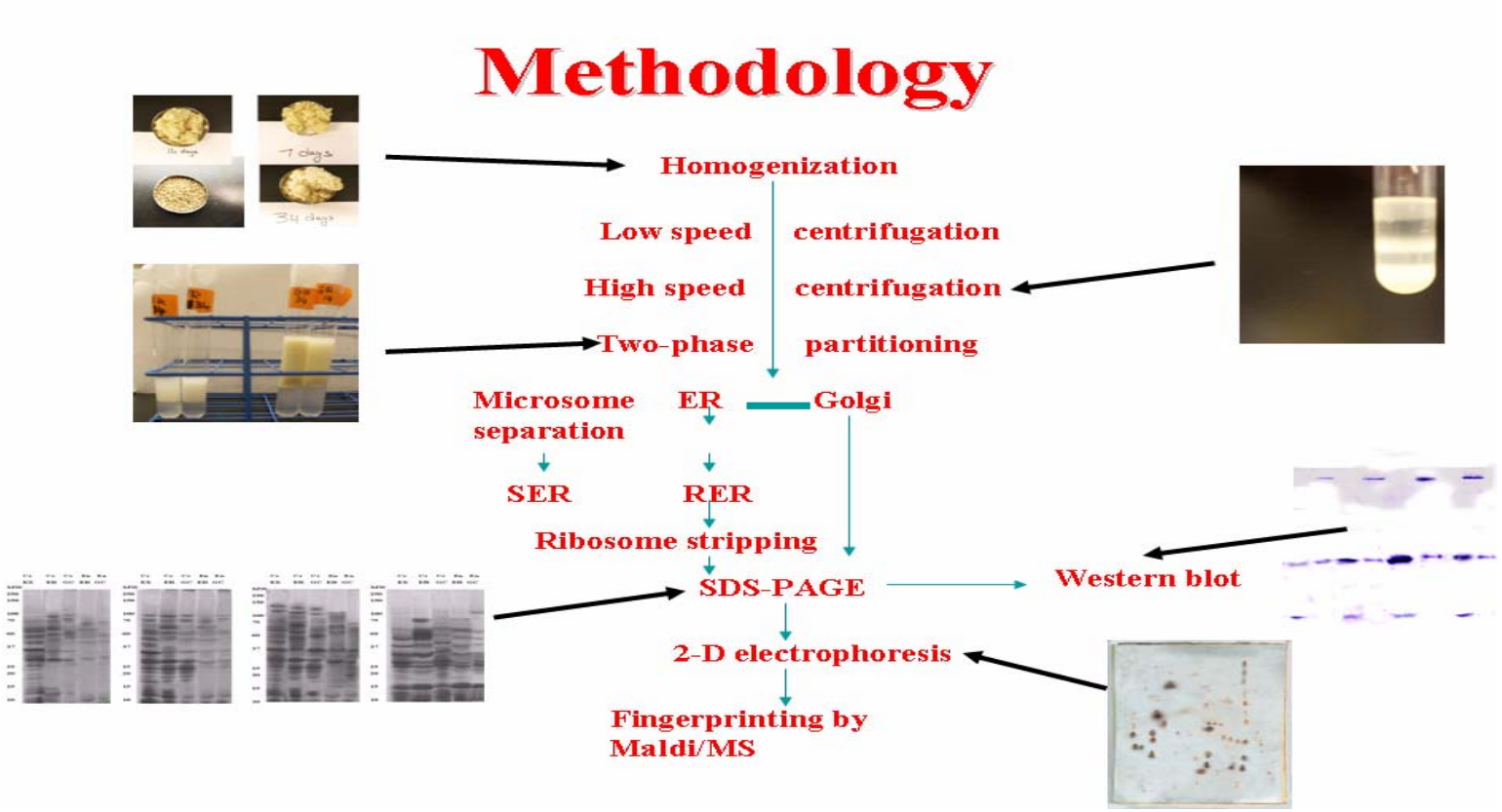

Fig. 5 Chart illustrating different steps of the fractionation and enrichment stages of ER and GC from wheat endosperm

VITA

Mohamad Aref El-Osta

Candidate for the Degree of

Doctoral of Philosophy

Thesis: A METHOD OF ENRICHMENT OF THE ENDOPLASMIC RETICULUM AND GOLGI COMPLEX PROTEINS FROM WHEAT SEEDS (*TRITICUM AESTIVUM*) AT DIFFERENT STAGES OF GROWTH

Major Field: Biochemistry and Molecular Biology

Biographical:

Personal Data: Born in Beirut, Lebanon, on august 17, 1965, the son of Dr. Aref and Huda El-Osta

Education: Received a Bachelor of Science degree in Food Technology from the American University of Beirut, Beirut Lebanon in July 1991. Awarded a diploma in Food Handling and Safety Inspection from the Royal Institute of Public Health and Hygiene, Portland Place, United Kingdom in March 1993. Awarded a Diploma in Quality University Instruction from Oklahoma State University, Stillwater, Oklahoma in December 1998. Awarded a Masters of Science degree with a major in Nutritional Sciences from Oklahoma State University, Stillwater Oklahoma in May 1999. Completed the requirement for the degree of Doctoral of Philosophy with a major in Biochemistry and Molecular Biology from Oklahoma State University, Stillwater Oklahoma in May 2005.

Professional experience: Research assistant, Department of Nutritional Sciences, Oklahoma State University, 1997-1999. Research assistant, Department of Biochemistry and Molecular Biology, 2000-2005

Name: Mohamad El-Osta Date of Degree: May 2005

Institution: Oklahoma State University Location: Stillwater, Oklahoma

Title of the Study: A METHOD OF ENRICHMENT OF THE ENDOPLASMIC RETICULUM AND GOLGI COMPLEX PROTEINS FROM WHEAT SEEDS (*TRITICUM AESTIVUM*) AT DIFFERENT STAGES OF GROWTH

Pages in study: 124 Candidate for the Degree of Doctor of Philosophy

Major Field: Biochemistry and Molecular Biology

Scope of study: Bread wheat (*Triticum aestivum*) is an important economic crop in the US and the world and its quality is related to storage protein. This study attempts to describe the proteins associated with the endoplasmic reticulum (ER) and Golgi complex (GC) of wheat endosperm. These proteins can be later used to related different aspects of storage proteins synthesis during endosperm development. The rate of reserve materials accumulation varies during the grain filling stages of wheat (early, early-mid, late-mid and mature, 7, 14, 34 and 60 days after anthesis, DAA, respectively). The proteins of the ER and GC are speculated to undergo changes in function, and possibly a temporal change in protein expression during these stages. The temporal change in protein composition within these organelles may be related to wheat proteins quality. The objective of this study is to develop a methodology for enriching organelles fractions from endosperm wheat and identify the constitutive proteins of these organelles at different stages. Enriched ER and GC fractions were obtained by discontinuous sucrose gradient fractionation and two-phase partitioning. Proteins were separated by 2-D electrophoresis and identified by peptide mass fingerprinting MALDI-TOF and MS-FIT database search.

Findings: The non-linear change in seeds weight confirmed that grain filling passes through different stages, including a change in protein filling as shown by protein determination assay (53.4, 69.6 and 101.4 mg/ml in 7, 14, and 34 DAA respectively). The enrichment of ER and GC was confirmed by immunodetection of enzymes markers. In SDS-PAGE, the enriched organelles fractions showed a difference in protein bands distribution at 34 DAA compared to earlier fractions (above 75 kDa and between 15-20 kDa), suggesting a diversity in organelles functionality, possibly due to a shift in major functions from protein synthesis to storage. At various stages, both enriched ER and GC showed a trend of similarity at 30-35 kDa, possibly due to the presence of common transport-related proteins in both organelles. Despite the limited solubility of the organelles in 2-D electrophoresis, a total of 234 spots were separated, 85 (36%) of them were fingerprinted by the MALDI-TOF and database search. Some identified proteins were markers for specific stages of development as PDI, starch synthase and nucellin-like aspartic protease.

Supervisor's Approval: Patricia Rayas-Duarte